Journal of Computational Physics **177,** 176–205 (2002)
doi:10.1006/jcph.2002.7009, available online at http://www.idealibrary.com on IDEAL®

Semirelativistic Magnetohydrodynamics and Physics-Based Convergence Acceleration

Tamas I. Gombosi,* Gábor Tóth,† Darren L. De Zeeuw,* Kenneth C. Hansen,* Konstantin Kabin,* and Kenneth G. Powell*

*Center for Space Environment Modeling, University of Michigan, Ann Arbor, Michigan, 48109-2143,
†Center for Space Environment Modeling, University of Michigan, Ann Arbor, Michigan, 48109-2143,
and Department of Atomic Physics, Loránd Eötvös University, Budapest, Hungary
E-mail: tamas@umich.edu, gtoth@umich.edu, darrens@umich.edu, kenhan@umich.edu,
kabin@phys.ualberta.ca, and powell@umich.edu

Received March 13, 2001; revised December 10, 2001

We derive a system of equations for semirelativistic magnetohydrodynamics (MHD) in which the bulk speed and the sound speed of the plasma are nonrelativistic, but the Alfvén speed can be relativistic. The characteristic wave speeds of the modified equation set are determined and compared to the wave speeds in "classical" (MHD). The stability conditions of the semirelativistic MHD equations are also investigated in detail.

This form of the MHD equations has a use beyond modeling flows with high Alfvén speeds. Even in cases with moderate Alfvén speeds, the semirelativistic form or certain approximations of it can be used to achieve accelerated numerical convergence to steady-state solutions by artificially reducing the speed of light, provided that the steady-state solutions of these equations are fully independent of the speed of light. Numerical tests are presented that demonstrate the behavior of solutions at high Alfvén speeds and the convergence acceleration that can be achieved when a steady-state solution is desired.

1. INTRODUCTION

The Alfvén speed in nonrelativistic magnetohydrodynamics (MHD) is defined as $V_A = B/\sqrt{\mu_0 \rho}$, where B is the magnitude of the magnetic field, ρ is the plasma mass density, and μ_0 is the permeability of vacuum. In some space plasmas V_A can evaluate to speeds larger than the speed of light, c. For example, in the near-Earth auroral zone of the terrestrial magnetosphere V_A is of the order of the speed of light, while in Jupiter's polar regions V_A/c can reach 10 or more. In such situations nonrelativistic MHD clearly loses validity.

In this paper we consider a semirelativistic set of MHD equations that combines nonrelativistic fluid dynamics with a fully relativistic treatment of the equations of electrodynamics.

0021-9991/02 $35.00

In essence this means that the displacement current and the electric force acting on the charge density are not neglected when the MHD equations are derived. Some of these modified equations were derived a long time ago and extensively investigated by Boris [2]. He showed that by keeping the displacement current the wave speeds of the semirelativistic equations become bounded by the speed of light in the plasma frame. This observation led Boris to suggest another possible use of the semirelativistic MHD equations: by artificially lowering the value of c one can reduce the wave speeds, which in turn allows bigger time steps for explicit numerical schemes. Both the semirelativistic corrections of classical MHD equations and the idea of artificially lowering the speed of light are known in the MHD community as the "Boris correction."

The semirelativistic MHD equations in their simplest nonconservative form involve c in two terms only: the displacement current $(1/\mu_0 c^2)(\partial \mathbf{E}/\partial t)$ and the electric force $(1/\mu_0 c^2)\mathbf{E}\nabla \cdot \mathbf{E}$ acting on the charge density. In steady-state solutions all time derivatives vanish; thus the value of c in the displacement current can be treated as a free parameter and can artificially be lowered without changing the final steady-state solution. Consequently the semirelativistic MHD equations with an artificially lowered speed of light can be used as a physics-based acceleration technique toward steady state. We note already here that the c parameter in the charge density should not be changed (since the electric acceleration force does not vanish in steady state), which results in a source term that has not been considered previously. When the semirelativistic MHD equations are used with a reduced speed of light, the stability of the equations becomes nontrivial.

There are various simplified forms of the semirelativistic MHD equation that can also be used for acceleration to a steady state. One version proposed by Boris differs from the nonrelativistic MHD equations only in the time derivative of the momentum, where the momentum is multiplied with a coefficient $\gamma_A^{-2} = 1 + V_A^2/c^2$. This modification is fully conservative and the steady state is independent of the speed of light, because it only occurs in a time derivative. Another type of approximation uses the primitive nonconservative form of the MHD equations and multiplies the Lorentz force $\mathbf{j} \times \mathbf{B}$ by a factor γ_A^2. This form has been used for many years, for both steady state and time accurate applications (e.g., [13, 18, 23]), although in this case the steady state is not independent of the speed of light. We will examine the wave speeds and the stability of these simplified forms of the semirelativistic MHD equations as well.

The reduced speed of light acceleration technique may even apply to certain time-accurate calculations. If the simulation domain consists of a dynamic part, in which even the lowered speed of light c is much larger than the wave speeds, and a quasi-stationary part, in which the wave speeds are limited by c, the solution is likely to be unaffected by the acceleration. Such a situation is typical in some magnetospheric simulations, in which the time step is limited by the extremely large wave speeds close to the magnetized body where the flow is essentially stationary, while far from the body there are dynamic variations but the wave speeds are orders of magnitude lower.

The paper is organized as follows. In Section 2 we derived the semirelativistic MHD equations in various forms. We also briefly discuss some simplified forms. The wave speeds and the stability of the semirelativistic MHD equations are examined in Sections 3 and 4. Section 5 gives the wave speeds for two of the simplified forms of the semirelativistic equations. The splitting of the magnetic field into an analytic $\mathbf{B}_0$ term and a deviation $\mathbf{B}_1$ term (introduced for classical MHD by Ogino and Walker [15] and later applied to Godunov-type schemes by Tanaka [20]) is generalized to the semirelativistic

case in Section 6. Numerical tests are presented in Section 7 and we conclude with Section 8.

2. SEMIRELATIVISTIC MHD EQUATIONS

2.1. Relativistic MHD in the Low-Speed Limit

To derive the semirelativistic MHD equations, we start with the conservative form of the relativistic MHD equations [9–11],

$$\frac{\partial \mathbf{W}}{\partial t} + (\nabla \cdot \mathbf{F})^{\mathrm{T}} = \mathbf{0}, \tag{1}$$

where the state vector, $\mathbf{W}$, and the flux diad, $\mathbf{F}$, are

$$\mathbf{W} = \begin{pmatrix} \Gamma \rho \\ \Gamma^2 \frac{e+p}{c^2}\mathbf{u} + \frac{1}{c^2}\mathbf{S}_{\mathrm{A}} \\ \mathbf{B} \\ \Gamma^2(e+p) - p - \Gamma\rho c^2 + e_{\mathrm{A}} \end{pmatrix} \tag{2}$$

and

$$\mathbf{F} = \begin{pmatrix} \Gamma\rho\mathbf{u} \\ \frac{\Gamma^2}{c^2}(e+p)\mathbf{u}\mathbf{u} + p\mathbf{I} + \mathbf{P}_{\mathrm{A}} \\ \mathbf{u}\mathbf{B} - \mathbf{B}\mathbf{u} \\ [\Gamma^2(e+p) - \Gamma\rho c^2]\mathbf{u} + \mathbf{S}_{\mathrm{A}} \end{pmatrix}^{\mathrm{T}}. \tag{3}$$

In Eqs. (2) and (3) we used the following definitions:

$$\Gamma = \frac{1}{\sqrt{1 - \frac{u^2}{c^2}}}, \tag{4}$$

$$\mathbf{S}_{\mathrm{A}} = \frac{1}{\mu_0}(\mathbf{E} \times \mathbf{B}), \tag{5}$$

$$e_{\mathrm{A}} = \frac{1}{2\mu_0}\left(B^2 + \frac{1}{c^2}E^2\right), \tag{6}$$

$$\mathbf{P}_{\mathrm{A}} = e_{\mathrm{A}}\mathbf{I} - \frac{1}{\mu_0}\mathbf{B}\mathbf{B} - \frac{1}{\mu_0 c^2}\mathbf{E}\mathbf{E}. \tag{7}$$

Here Γ, $\mathbf{S}_{\mathrm{A}}$, e_{A}, and $\mathbf{P}_{\mathrm{A}}$ are the Lorentz factor, the Poynting vector, the electromagnetic energy density, and the electromagnetic pressure tensor, respectively. Furthermore, $\mathbf{I}$ is the 3 by 3 identity matrix and $\mathbf{E} = -\mathbf{u} \times \mathbf{B}$ is the motional electric-field vector. In the relativistic MHD equations ρ, p, and e are the mass density, the pressure, and the internal (thermal and rest mass) energy density in the local rest frame of the fluid. The plasma pressure is the sum of the electron and ion pressures, $p = p_e + p_i$. It should be emphasized that one must use a relativistic equation of state to define the energy density e. For relativistic, perfect gases the relativistic form of the Maxwell–Boltzmann distribution must be used and the equation of state becomes substantially more complicated [8]. Finally, we note that p is frame invariant and that the transformation of ρ to the laboratory frame is $\rho_L = \Gamma\rho$.

Next we take the semirelativistic limit of (1). This limit is obtained by assuming that the plasma flow itself is nonrelativistic, but keeping the full relativistic form of the electromagnetic terms. Mathematically speaking, we assume that both the bulk speed u and the sound speed $a = \sqrt{\gamma p/\rho}$ (where γ is the specific heat ratio) are nonrelativistic ($u, a \ll c$); therefore the internal energy becomes

$$e = \rho c^2 + \frac{p}{\gamma - 1}, \tag{8}$$

which includes the thermal energy density and the energy density associated with the rest mass. Second-order terms in u/c and a/c are dropped only when a similar zeroth-order term is present. This is quite straightforward and requires care only when Γ or Γ^2 is multiplied by a term including ρc^2. In this case we must use $\Gamma \approx 1 + u^2/(2c^2)$; otherwise we simply use the stronger limit $\Gamma \to 1$. Applying these limits and keeping the electromagnetic terms intact yields

$$\mathbf{W} = \begin{pmatrix} \rho \\ \rho\mathbf{u} + \frac{1}{c^2}\mathbf{S}_\mathrm{A} \\ \mathbf{B} \\ \frac{1}{2}\rho u^2 + \frac{p}{\gamma-1} + e_\mathrm{A} \end{pmatrix}, \tag{9}$$

$$\mathbf{F} = \begin{pmatrix} \rho\mathbf{u} \\ \rho\mathbf{u}\mathbf{u} + p\mathbf{I} + \mathbf{P}_\mathrm{A} \\ \mathbf{u}\mathbf{B} - \mathbf{B}\mathbf{u} \\ \left(\frac{1}{2}\rho u^2 + \frac{\gamma p}{\gamma-1}\right)\mathbf{u} + \mathbf{S}_\mathrm{A} \end{pmatrix}^\mathrm{T}. \tag{10}$$

In semirelativistic MHD, Eq. (1) is solved with the state vector and flux diad given by expressions (9) and (10).

In a scheme based on the semirelativistic MHD equation, it is necessary to convert the vector of conserved variables $\mathbf{W}$ in (9) to the primitive variables. The only nontrivial transformation involves the semirelativistic momentum

$$\mathbf{m} = \rho\mathbf{u} + \frac{1}{c^2}\mathbf{S}_\mathrm{A} = \rho\mathbf{u} - \frac{1}{\mu_0 c^2}(\mathbf{u} \times \mathbf{B}) \times \mathbf{B}. \tag{11}$$

Using some vector identities and $V_\mathrm{A}^2 = \mathbf{B}^2/(\mu_0\rho)$, the semirelativistic momentum can be rewritten as

$$\mathbf{m} = \left[\mathbf{I} + \frac{V_\mathrm{A}^2}{c^2}(\mathbf{I} - \mathbf{b}\mathbf{b})\right] \cdot (\rho\mathbf{u}), \tag{12}$$

where we introduced the unit vector parallel with the magnetic field

$$\mathbf{b} = \frac{\mathbf{B}}{|\mathbf{B}|}. \tag{13}$$

The matrix multiplying $\rho\mathbf{u}$ in (12) can be inverted to give

$$\left[\mathbf{I} + \frac{V_\mathrm{A}^2}{c^2}(\mathbf{I} - \mathbf{b}\mathbf{b})\right]^{-1} = \gamma_\mathrm{A}^2\left[\mathbf{I} + \frac{V_\mathrm{A}^2}{c^2}\mathbf{b}\mathbf{b}\right], \tag{14}$$

where we introduced the Alfvén factor

$$\gamma_A = \frac{1}{\sqrt{1 + \frac{V_A^2}{c^2}}}. \tag{15}$$

Finally, the transformation from the semirelativistic momentum to the nonrelativistic momentum becomes

$$\rho \mathbf{u} = \gamma_A^2 \left[\mathbf{I} + \frac{V_A^2}{c^2} \mathbf{bb} \right] \cdot \mathbf{m}. \tag{16}$$

2.2. MHD with Displacement Current and Charge Density

An alternative derivation leading to the semirelativistic MHD equations starts with the nonconservative form of the nonrelativistic MHD equations but with the electric force in the momentum equation and the displacement current in Ampére's law being kept. A form of this derivation was discussed by Boris [2]. In this case the governing equations are

$$\frac{\partial \rho}{\partial t} + (\mathbf{u} \cdot \nabla)\rho + \rho(\nabla \cdot \mathbf{u}) = 0, \tag{17}$$

$$\rho \frac{\partial \mathbf{u}}{\partial t} + \rho(\mathbf{u} \cdot \nabla)\mathbf{u} + \nabla p - \mathbf{j} \times \mathbf{B} - q\mathbf{E} = 0, \tag{18}$$

$$\frac{\partial \mathbf{B}}{\partial t} + \nabla \times \mathbf{E} = 0, \tag{19}$$

$$\frac{\partial p}{\partial t} + (\mathbf{u} \cdot \nabla)p + \gamma p(\nabla \cdot \mathbf{u}) = 0, \tag{20}$$

where the charge density q, the current density $\mathbf{j}$, and the electric field vector $\mathbf{E}$ are defined by *Gauss's law, Ampère's law*, and *Ohm's law*, respectively:

$$q = \frac{1}{\mu_0 c^2} \nabla \cdot \mathbf{E}, \tag{21}$$

$$\mathbf{j} = \frac{1}{\mu_0} \nabla \times \mathbf{B} - \frac{1}{\mu_0 c^2} \frac{\partial \mathbf{E}}{\partial t}, \tag{22}$$

$$\mathbf{E} = -\mathbf{u} \times \mathbf{B}. \tag{23}$$

Now the $\mathbf{j} \times \mathbf{B}$ term can be expressed from (22). We use the $(\partial \mathbf{E}/\partial t) \times \mathbf{B} = \partial(\mathbf{E} \times \mathbf{B})/\partial t - \mathbf{E} \times (\partial \mathbf{B}/\partial t)$ identity and then $\partial \mathbf{B}/\partial t$ is substituted from the induction equation (19). After some algebra we obtain

$$\mathbf{j} \times \mathbf{B} = -\frac{1}{c^2} \frac{\partial \mathbf{S}_A}{\partial t} - \nabla \cdot \mathbf{P}_A - \frac{1}{\mu_0 c^2} \mathbf{E} \nabla \cdot \mathbf{E}. \tag{24}$$

Substituting Eqs. (17), (21), and (24) into (18) yields the conservative form of the momentum equation

$$\frac{\partial}{\partial t} \left(\rho \mathbf{u} + \frac{1}{c^2} \mathbf{S}_A \right) + \nabla \cdot (\rho \mathbf{u}\mathbf{u} + p\mathbf{I} + \mathbf{P}_A) = 0, \tag{25}$$

which is identical to the momentum equations in (9) and (10) that were derived from the relativistic MHD equations.

2.3. Divergence of the Magnetic Field

In nature $\nabla \cdot \mathbf{B}$ is always zero; i.e., magnetic monopoles do not exist. Mathematically speaking, if the $\nabla \cdot \mathbf{B} = 0$ condition is satisfied initially, it will hold forever, since the induction equation (19) ensures that $\partial(\nabla \cdot \mathbf{B})/\partial t = 0$. Many numerical discretizations of the MHD equations, however, lead to a nonzero $\nabla \cdot \mathbf{B}$ in the discretized solution due to the truncation errors, even if the initial condition is divergence free. Other schemes enforce the divergence-free condition in some discrete sense. Many of these schemes were described and compared by Tóth [21].

For schemes that allow nonzero $\nabla \cdot \mathbf{B}$ at the truncation error level, it is beneficial to use a form of the MHD equations that includes the effects of magnetic monopoles. A Galilean invariant form of the nonrelativistic MHD equations, in which the magnetic monopoles are advected with the bulk flow, was derived by Godunov [5] and later implemented and tested by Powell and co-workers [16, 17]. In this "8-wave" formulation, the nonrelativistic MHD equations are written in a near conservation form, with source terms proportional to $\nabla \cdot \mathbf{B}$ in the momentum, induction, and energy equations. The 8th wave corresponds to the propagation of the magnetic monopoles, or in other words, jumps in the normal component of the magnetic field.

In recent papers by Janhunen [7] and Dellar [3] it was shown that if one starts from the relativistic MHD equations, which allow the existence of magnetic monopoles, while the momentum and energy equations remain in conservation form. In the induction equation one can introduce the same source term $-\mathbf{u}\nabla \cdot \mathbf{B}$ as in the 8-wave scheme to allow for the advection of magnetic monopoles. This set of equations is Lorentz invariant. Another interesting alternative can be obtained by artifically diffusing the magnetic monopoles with a source term proportional to $\nabla(\nabla \cdot \mathbf{B})$ in the induction equation. This can be achieved with the method proposed by Marder [14].

Clearly, one can prescribe anything for the numerically generated monopoles, as long as it makes the numerical scheme more stable and hopefully more accurate. All the above ideas can be easily carried over to the semirelativistic MHD equations. In particular, the induction equation is the same as in the nonrelativistic case; thus the same source terms can be applied. It is a question of numerical experiments to decide which form of the source terms make a certain discretization of the semirelativistic MHD equations behave the best.

2.4. Acceleration toward Steady State with Lowered Speed of Light

So far our aim has been to derive a set of equations that is valid in physical situations in which $V_A > c$. However, we also want a set of equations which has steady-state solutions independent of the value of the speed of light, since the artificial lowering of c allows larger time steps in the numerical simulations. This leads us to differentiate the true value of the speed of light, c_0, from the artificially lowered speed of light, c.

The flux diad (10) contains the speed of light only in the momentum equation in the term P_A. The divergence of these electric terms can be manipulated as follows:

$$\nabla \cdot \left[\frac{1}{\mu_0 c_0^2}\left(\frac{1}{2}E^2 - \mathbf{EE}\right)\right] = \nabla \cdot \left[\frac{1}{\mu_0 c^2}\left(\frac{1}{2}E^2 - \mathbf{EE}\right)\right] + \frac{1}{\mu_0}\left(\frac{1}{c_0^2} - \frac{1}{c^2}\right)[\mathbf{E} \times (\nabla \times \mathbf{E}) - \mathbf{E}\nabla \cdot \mathbf{E}]. \quad (26)$$

The first term on the right-hand side is the same as the left-hand side except for the reduced speed of light. For steady-state problems, we can make use of the steady-state induction equation, which yields $\nabla \times \mathbf{E} = 0$; thus the $\mathbf{E} \times (\nabla \times \mathbf{E})$ term vanishes from the second term on the right-hand side. In general, when the acceleration technique is applied with $c < c_0$, we need to solve the near conservation equation

$$\frac{\partial \mathbf{W}}{\partial t} + (\nabla \cdot \mathbf{F})^{\mathrm{T}} = \mathbf{Q}, \tag{27}$$

where the source term is

$$\mathbf{Q} = \frac{1}{\mu_0}\left(\frac{1}{c_0^2} - \frac{1}{c^2}\right)\mathbf{E}\nabla \cdot \mathbf{E} \tag{28}$$

in the momentum equation. This source term compensates for the change due to lowering c.

Another way of deriving (27) and (28) is to realize that the steady-state solution of the semirelativistic MHD equations is independent of the displacement current $(1/\mu_0 c^2)\partial \mathbf{E}/\partial t$, but it does depend on the charge density $(1/\mu_0 c^2)\nabla \cdot \mathbf{E}$. Therefore the speed of light can be freely reduced in Ampére's law (22) but it must be kept at $c = c_0$ in Gauss's law (21). Consequently, the $(1/\mu_0 c^2)\mathbf{E}\nabla \cdot \mathbf{E}$ term from (24) and the $(1/\mu_0 c_0^2)\mathbf{E}\nabla \cdot \mathbf{E}$ term from (21) do not cancel as they did in the momentum equation (25).

2.5. Split Hydrodynamic/Electromagnetic Form

In some popular numerical methods (e.g., [4]) the hydrodynamics is treated in a flux-based form, with the electromagnetic terms split out and treated as a source term. In this section we consider the semirelativistic MHD equations in this formulation.

In the split hydrodynamic/electromagnetic formulation the continuity equation and Faraday's law are given by (17) and (19). To derive an appropriate momentum equation we substitute Ohm's law (23) into Ampère's law (22), evaluate the $\partial \mathbf{B}/\partial t$ term from the induction equation (19), and take the cross product with $\mathbf{B}$ to obtain

$$\mathbf{j} \times \mathbf{B} = -\frac{1}{\mu_0 c^2}(B^2\mathbf{I} - \mathbf{BB}) \cdot \frac{\partial \mathbf{u}}{\partial t} - \frac{\mathbf{1}}{\mu_0}\mathbf{B} \times \left[\nabla \times \mathbf{B} + \frac{1}{c^2}(\nabla \times \mathbf{E}) \times \mathbf{u}\right]. \tag{29}$$

Substituting (29) into the momentum equation (18) yields

$$\rho\left[\mathbf{I} + \frac{V_{\mathrm{A}}^2}{c^2}(\mathbf{I} - \mathbf{bb})\right] \cdot \frac{\partial \mathbf{u}}{\partial t} + \rho(\mathbf{u} \cdot \nabla)\mathbf{u} + \nabla p + \frac{1}{\mu_0}\mathbf{B} \times \left[\nabla \times \mathbf{B} + \frac{1}{c^2}(\nabla \times \mathbf{E}) \times \mathbf{u}\right] - q\mathbf{E} = 0. \tag{30}$$

We find the same matrix multiplying the $\partial \mathbf{u}/\partial t$ term as in (12), and so (30) can be multiplied with the inverse matrix (14) to obtain the split hydrodynamic/electromagnetic form of the MHD momentum equation,

$$\frac{\partial}{\partial t}(\rho \mathbf{u}) + \nabla \cdot (\rho \mathbf{uu} + p\mathbf{I}) = \gamma_{\mathrm{A}}^2 \frac{V_{\mathrm{A}}^2}{c^2}(\mathbf{I} - \mathbf{b}\,\mathbf{b}) \cdot [\rho(\mathbf{u} \cdot \nabla)\mathbf{u} + \nabla p] - \gamma_{\mathrm{A}}^2 \frac{1}{\mu_0}\mathbf{B} \times \left[\nabla \times \mathbf{B} - \frac{1}{c^2}\mathbf{u} \times (\nabla \times \mathbf{E}) - \frac{1}{c_0^2}\mathbf{u}\nabla \cdot \mathbf{E}\right], \tag{31}$$

where the continuity equation (17) was used to convert from the time derivative of velocity to the time derivative of momentum. We note that the terms on the right-hand side are all perpendicular to the magnetic-field direction. This point will be discussed later.

The split hydrodynamic/electromagnetic form of the energy equation can be obtained by combining Eqs. (31) and (20) to give

$$\frac{\partial \varepsilon}{\partial t} + \nabla \cdot [(\varepsilon + p)\mathbf{u}] = \gamma_{\mathrm{A}}^2 \frac{V_{\mathrm{A}}^2}{c^2} (\mathbf{I} - \mathbf{bb}) : [\rho \mathbf{u}(\mathbf{u} \cdot \nabla)\mathbf{u} + \mathbf{u}\nabla p] - \gamma_{\mathrm{A}}^2 \frac{1}{\mu_0} (\mathbf{u} \times \mathbf{B}) \cdot (\nabla \times \mathbf{B}), \tag{32}$$

where the : symbol means the double dot product of the matrices, and the hydrodynamic energy density ε is defined as

$$\varepsilon = \frac{1}{2}\rho u^2 + \frac{p}{\gamma - 1}. \tag{33}$$

We note that in Eqs. (31) and (32) no additional simplification has been used beyond the semirelativistic approximation.

2.6. Primitive-Variable Form

In the primitive-variable formulation (17) through (19) of the semirelativistic MHD equations only the momentum equation is modified due to the displacement curent. Multiplying Eq. (30) with the inverse matrix (14) yields the following equation for the evolution of plasma flow velocity:

$$\frac{\partial \mathbf{u}}{\partial t} + \gamma_{\mathrm{A}}^2 \left(\mathbf{I} + \frac{V_{\mathrm{A}}^2}{c^2} \mathbf{b}\,\mathbf{b} \right) \cdot \left[(\mathbf{u} \cdot \nabla)\mathbf{u} + \frac{1}{\rho} \nabla p \right] + \gamma_{\mathrm{A}}^2 \frac{1}{\mu_0 \rho} \mathbf{B} \times \left[\nabla \times \mathbf{B} - \frac{1}{c^2} \mathbf{u} \times (\nabla \times \mathbf{E}) - \frac{1}{c_0^2} \mathbf{u} \nabla \cdot \mathbf{E} \right] = 0. \tag{34}$$

The primitive-variable set of the semirelativistic MHD equations are (17), (34), (20), and (19), together with Ohm's law (23).

2.7. The Semirelativistic Momentum Equation

In this section we examine some interesting features of the semirelativistic momentum equation (34). We note, again, that in the primitive-variable formulation this is the only equation modified by the semirelativistic effects.

Parallel and perpendicular components. Equation (34) can be examined by considering the parallel and perpendicular components, with respect to the magnetic field, separately. Let us start by taking the scalar product of (34) with **b**,

$$\left(\frac{\partial u}{\partial t} \right)_{\parallel} + \left[(\mathbf{u} \cdot \nabla)\mathbf{u} + \frac{1}{\rho} \nabla p \right]_{\parallel} = 0, \tag{35}$$

where the subscript $\parallel$ denotes the magnetic-field-aligned component. This equation means that the plasma transport along the magnetic field line is completely hydrodynamic. The

magnetic field does not influence this field-aligned transport and the semirelativistic approximation results in no modification whatsoever.

The situation is completely different in the perpendicular direction. This can be seen by multiplying Eq. (34) with the matrix $(\mathbf{I} - \mathbf{bb})$, which gives

$$\left(\frac{\partial \mathbf{u}}{\partial t}\right)_{\perp} + \gamma_A^2 \left[(\mathbf{u}\cdot\nabla)\mathbf{u} + \frac{1}{\rho}\nabla p\right]_{\perp} + \frac{\gamma_A^2}{\mu_0 \rho}\mathbf{B}\times\left[\nabla\times\mathbf{B} - \frac{1}{c^2}\mathbf{u}\times(\nabla\times\mathbf{E}) - \frac{1}{c_0^2}\mathbf{u}\nabla\cdot\mathbf{E}\right] = 0, \tag{36}$$

where the subscript $\perp$ denotes the component perpendicular to the magnetic field. This equation shows that the time rate of change of the flow velocity in the perpendicular direction is reduced by a factor of $\gamma_A^{-2} = 1 + V_A^2/c^2$. This can be interpreted as a consequence of an increase of the "generalized" mass density in the perpendicular direction by this factor. In effect, it is increasingly difficult to change the perpendicular velocity as the Alfvén speed increases, and as $V_A \to \infty$ all transverse oscillations become impossible.

Steady-state solution. It is expected that under steady-state conditions the semirelativistic MHD equations revert to the nonrelativistic case, since the displacement current is essentially the time rate of change of the electric field vector. The parallel component of the primitive-variable momentum equation has no semirelativistic terms, so the steady-state parallel velocity is obviously the same in both cases. Under steady-state conditions the perpendicular component (36) becomes

$$[\rho(\mathbf{u}\cdot\nabla)\mathbf{u} + \nabla p]_{\perp} + \frac{1}{\mu_0}\mathbf{B}\times(\nabla\times\mathbf{B}) - \frac{1}{\mu_0 c_0^2}\mathbf{E}\nabla\cdot\mathbf{E} = 0, \tag{37}$$

because one can use Eq. (19) to show that $\mathbf{u}\times(\nabla\times\mathbf{E})$ vanishes in steady state. Equation (37) is the same as the perpendicular component of the steady-state nonrelativistic momentum equation. This means that steady-state solutions of the nonrelativistic and semirelativistic MHD equations must be identical at the level of the partial-differential equations. Discrete solutions of the two forms can differ slightly, since discretization of the two forms will lead to different amounts of discretization error.

2.8. Approximate Equations

Next we examine two simplified approximations to the semirelativistic MHD equation. Neither of the simplifications is valid for truly semirelativistic problems, where $V_A > c$. The first simplified version proposed by Boris [2] can be used to obtain steady-state solutions of the nonrelativistic MHD equations with accelerated convergence. The second approximation has been used in practical simulations to overcome numerical difficulties, but the effects of the approximations even on the steady-state solution are not clear.

The Boris simplification. First we discuss an approximation that was put forward by Boris in his original paper [2]. Boris suggested neglecting the off-diagonal term $(b_i b_j)$ in the time derivative of the semirelativistic momentum, as well as the electric field contributions to the electromagnetic energy and pressure tensor. At the same time he used the nonconservative energy equation given by Eq. (20). This combination leads to a set of equations which cannot be expressed in conservation form. Here we consider a somewhat

modified approach, in which we use the conservative form of the semirelativistic energy equation but neglect the electric field contribution to the conserved energy density. This approximation results in a conservative state vector which has increased inertia compared to the nonrelativistic approximation. We note that while this approximation has some very attractive properties, the entropy function loses its usual physical meaning. In this approximation the state vector is modified but the flux diad becomes identical to the nonrelativistic case:

$$\mathbf{W}^{\mathrm{s}} = \begin{pmatrix} \rho \\ \left(1 + \frac{V_{\mathrm{A}}^2}{c^2}\right)\rho\mathbf{u} \\ \mathbf{B} \\ \frac{1}{2}\rho u^2 + \frac{p}{\gamma - 1} + \frac{1}{2\mu_0}B^2 \end{pmatrix}, \tag{38}$$

$$\mathbf{F}^{\mathrm{s}} = \begin{pmatrix} \rho\mathbf{u} \\ \rho\mathbf{u}\mathbf{u} + p\mathbf{I} + \frac{1}{2\mu_0}B^2\mathbf{I} - \frac{1}{\mu_0}\mathbf{B}\mathbf{B} \\ \mathbf{u}\mathbf{B} - \mathbf{B}\mathbf{u} \\ \left(\frac{1}{2}\rho u^2 + \frac{\gamma p}{\gamma - 1} + \frac{1}{\mu_0}B^2\right)\mathbf{u} - \frac{1}{\mu_0}(\mathbf{u}\cdot\mathbf{B})\mathbf{B} \end{pmatrix}^{\mathrm{T}}. \tag{39}$$

The only difference from the nonrelativistic MHD equations is the $1 + V_{\mathrm{A}}^2/c^2$ factor in front of $\rho\mathbf{u}$ in the vector of conservative variables W. Since the stationary solution of $\partial W/\partial t + \nabla\cdot\mathbf{F} = 0$ only depends on the fluxes $\mathbf{F}$, the steady-state solution is independent of the speed of light.

Reduced $\mathbf{j}\times\mathbf{B}$ *force.* An even simpler approximation can be obtained with the help of Eq. (34). One can neglect the electric field contributions to the $\mathbf{j}\times\mathbf{B}$ force and the relativistic reduction of the hydrodynamic forces to obtain the following approximation to the momentum equation:

$$\frac{\partial\mathbf{u}}{\partial t} + (\mathbf{u}\cdot\nabla)\mathbf{u} + \frac{1}{\rho}\nabla p + \gamma_{\mathrm{A}}^2\frac{1}{\mu_0\rho}\mathbf{B}\times(\nabla\times\mathbf{B}) = 0. \tag{40}$$

This equation is the "classic" MHD momentum equation with a reduced $\mathbf{j}\times\mathbf{B}$ force. The reduction resolves the stiffnes of the equation, since the modified $\mathbf{j}\times\mathbf{B}$ remains bounded as the magnetic field strength approaches infinity.

This approximation is very convenient and easy to implement in numerical codes. It is extensively used in global magnetospheric codes to avoid unphysical Alfvén speed ($V_{\mathrm{A}} > c$) and for increasing the explicit time step (with reduced values of c) [13]. We note, however, that (40) suffers from two shortcomings: it cannot be put in a conservation form, which would be important in obtaining discontinuous solutions, and the steady-state solution depends on the value of the reduced speed of light.

3. WAVE SPEEDS

In this section we determine how the MHD wave speeds are modified by the semirelativistic correction. Our starting point is the primitive-variable form of the semirelativistic

MHD equations (17), (34), (20), and (19), together with (23). The use of the primitive-variable form leads to a somewhat simpler eigenvalue problem than the one derived from the conservative form, thereby simplifying the analysis. We will also drop the $(1/c_0^2)\mathbf{u}\nabla\cdot\mathbf{E}$ term from (34), since it is negligible relative to $\nabla\times\mathbf{B}$, which is a factor $(c_0/u)^2$ larger. Dropping this term makes the eigenvalue problem much easier to treat analytically. Note that while $u \ll c_0$ always holds in the semirelativistic MHD limit, the $u \ll c$ condition may not be true when the speed of light is artificially reduced. Finally, we add a $-\mathbf{u}\nabla\cdot\mathbf{B}$ source term to the induction equation (19) so that the divergence wave has a nonzero wave speed. This source term removes the singularity of the matrix, but otherwise it has no influence on the other waves, which have no jump in the normal component of the magnetic field.

3.1. Characteristic Matrix of Semirelativistic MHD

The primitive-variable semirelativistic MHD equations can be written in a general quasi-linear form

$$\frac{\partial\mathbf{U}}{\partial t}+\mathbf{M}_x\frac{\partial\mathbf{U}}{\partial x}+\mathbf{M}_y\frac{\partial\mathbf{U}}{\partial y}+\mathbf{M}_z\frac{\partial\mathbf{U}}{\partial z}=0, \tag{41}$$

where $\mathbf{U}$ is the vector of primitive variables $(\rho, \mathbf{u}, \mathbf{B}, p)^{\mathrm{T}}$. If the eigenvalues of $\mathbf{M}_x$, $\mathbf{M}_y$, and $\mathbf{M}_z$ are all real (they need not be distinct and are typically not in systems of conservation laws), the system is hyperbolic. The eigenvalues of the matrices $\mathbf{M}_i$ represent the wave speeds in the given direction.

The characteristic matrix of the semirelativistic MHD equations in direction x is

$$\mathbf{M}_x=\begin{pmatrix}
u_x & \rho & 0 & 0 & 0 & 0 & 0 & 0\\
0 & \gamma_{\mathrm{A}}^2u_x+\chi_{xx} & \chi_{xy} & \chi_{xz} & \eta_{xx} & \eta_{xy} & \eta_{xz} & \kappa_x\\
0 & \chi_{yx} & \gamma_{\mathrm{A}}^2u_x+\chi_{yy} & \chi_{yz} & \eta_{yx} & \eta_{yy} & \eta_{yz} & \kappa_y\\
0 & \chi_{zx} & \chi_{zy} & \gamma_{\mathrm{A}}^2u_x+\chi_{zz} & \eta_{zx} & \eta_{zy} & \eta_{zz} & \kappa_z\\
0 & 0 & 0 & 0 & u_x & 0 & 0 & 0\\
0 & B_y & -B_x & 0 & 0 & u_x & 0 & 0\\
0 & B_z & 0 & -B_x & 0 & 0 & u_x & 0\\
0 & \rho a^2 & 0 & 0 & 0 & 0 & 0 & u_x
\end{pmatrix}, \tag{42}$$

where

$$\chi=\frac{\gamma_{\mathrm{A}}^2}{\mu_0\rho c^2}\begin{pmatrix}
2B_x^2u_x-B^2u_x & 2B_xB_yu_x & 2B_xB_zu_x\\
2B_xB_yu_x+B_zE_x & 2B_y^2u_x-B^2u_x+B_zE_y & 2B_yB_zu_x+B_zE_z\\
2B_xB_zu_x-B_yE_x & 2B_yB_zu_x-B_yE_y & 2B_z^2u_x-B^2u_x-B_yE_z
\end{pmatrix},$$

$$\eta=\frac{\gamma_{\mathrm{A}}^2}{\mu_0\rho c^2}\begin{pmatrix}
u_x\mathbf{u}\cdot\mathbf{B}-u_x^2B_x & (c^2-u_x^2)B_y & (c^2-u_x^2)B_z\\
-u_xu_yB_x & u_x\mathbf{u}\cdot\mathbf{B}-u_xu_yB_y-c^2B_x & u_xu_yB_z\\
-u_xu_zB_x & -u_xu_zB_y & u_x\mathbf{u}\cdot\mathbf{B}-u_xu_zB_z-c^2B_x
\end{pmatrix}, \tag{43}$$

$$\kappa=\frac{\gamma_{\mathrm{A}}^2}{\rho}\left(1+\frac{V_{\mathrm{A}_x}^2}{c^2};\frac{V_{\mathrm{A}_x}V_{\mathrm{A}_y}}{c^2};\frac{V_{\mathrm{A}_x}V_{\mathrm{A}_z}}{c^2}\right)^{\mathrm{T}},$$

and $V_{A,x}$, $V_{A,y}$, and $V_{A,z}$ are the components of the nonrelativistic Alfvén speed, eg., $V_{A,x} = B_x/\sqrt{\mu_0\rho}$. The wave speeds, i.e., the eigenvalues of the M_x matrix (42), are the roots of the characteristic equation

$$(\lambda - u_x)^2 P_2(\lambda) P_4(\lambda) = 0, \tag{44}$$

where P_2 and P_4 are second- and fourth-order polynomials

$$P_2 = \lambda(\lambda - u_x) + \gamma_A^2 \left[\lambda u_\parallel b_x \frac{V_A^2}{c^2} - u_x(\lambda - u_x) - V_A^2 b_x^2 \right], \tag{45}$$

$$P_4 = [(\lambda - u_x)^4 - a^2(\lambda - u_x)^2] - (c^2 - \lambda^2)\frac{V_A^2}{c^2}\left[(\lambda - u_x)^2 - a^2 b_x^2\right], \tag{46}$$

where $u_\parallel = \mathbf{u} \cdot \mathbf{b}$. Two of the roots of Eq. (44) are trivial:

$$\lambda_{1,2} = u_x. \tag{47}$$

These eigenvalues describe the entropy wave and the $\nabla \cdot \mathbf{B}$ wave [19] and are not modified by the semirelativistic MHD approximation. The $\nabla \cdot \mathbf{B}$ wave propagates the jump in the normal component of the magnetic field. The interpretation of this wave has been extensively discussed by our group [16, 17, 19].

3.2. Alfvén Waves

The two roots of P_2 correspond to the Alfén waves in the semirelativistic approximation,

$$\lambda_{3,4} = \gamma_A^2(u_x + v_{E,x}) \pm \sqrt{\gamma_A^2\left(V_{A,x}^2 - u_x^2\right) + \gamma_A^4 (u_x + v_{E,x})^2}, \tag{48}$$

where we have introduced the "Poynting velocity" as

$$\mathbf{v}_E = \frac{1}{2\rho c^2}\mathbf{S}_A = \frac{1}{2\mu_0\rho c^2}(\mathbf{E} \times \mathbf{B}) = \frac{V_A^2}{2c^2}\mathbf{u}_\perp, \tag{49}$$

where $\mathbf{u}_\perp = \mathbf{u} - u_\parallel \mathbf{b}$.

In the semirelativistic limit the Alfvén speeds are quite different than they are in classical MHD. One of the most striking features of these wave speeds is that they are not symmetric around the normal flow velocity component, u_x. This is a major difference from the classical nonrelativistic case, in which all wave speeds are symmetric with respect to u_x. This difference occurs because the semirelativistic MHD equations show a mixed translational invariance: the hydrodynamic part is Galilean invariant, while the electrodynamic part is Lorentz invariant. The end result is that the semirelativistic wave speeds show neither Galilean nor Lorentz invariance. It is interesting to note that the semirelativistic Alfvén waves symmetrically propagate forward and backward with respect to the modified bulk speed $\mathbf{u}' = \gamma_A^2(\mathbf{u} + \mathbf{v}_E)$.

It is instructive to investigate the Alfvén speeds in various limits. First we take the nonrelativistic limit $V_A \ll c$, $\gamma_A \to 1$, $v_E \to 0$ and obtain the classical MHD Alfvén speed

$$\lim_{V_A \ll c} \lambda_{3,4} = u_x \pm V_{A,x}, \tag{50}$$

as expected.

Next we examine the semirelativistic Alfvén speed in the plasma frame, $u_x = 0$, $\mathbf{v}_E = 0$:

$$\lim_{u_x \to 0} \lambda_{3,4} = \pm \gamma_A V_{A,x}. \tag{51}$$

This is identical to the Alfvén speeds derived by Boris [2].

Other interesting cases are when the magnetic field is perpendicular to ($b_x = 0$) or parallel with ($b_x = 1$) the propagation direction:

$$\lim_{b_x \to 0} \lambda_3 = u_x \quad \text{and} \quad \lim_{b_x \to 0} \lambda_4 = \gamma_A^2 u_x, \tag{52}$$

$$\lim_{b_x \to 1} \lambda_{3,4} = \gamma_A^2 u_x \pm \gamma_A V_A \sqrt{1 - \gamma_A^2 \frac{u_x^2}{c^2}}. \tag{53}$$

Another very important and interesting limit is when the classical Alfvén speed approaches infinity, $V_A \to \infty$. In this case $\gamma_A \to 0$ but $\gamma_A V_A \to c$ and the eigenvalues become

$$\lim_{V_A \to \infty} \lambda_{3,4} = \frac{1}{2} u_{\perp,x} \pm \sqrt{c^2 b_x^2 + \frac{1}{4} u_{\perp,x}^2}. \tag{54}$$

It is easy to see that the maximum value of the Alfvén speed is limited by $c + u$ in any frame of reference.

3.3. Fast and Slow Magnetosonic Waves

The fast and slow magnetosonic speeds are the roots of the $P_4 = 0$ equation. While the P_4 polynomial looks deceptively simple, its roots are very complicated. In order to explore the physics of these modified waves we first examine several simplified cases.

3.3.1. *Special Cases*

Zero flow velocity. Let us start the analysis of the magnetosonic waves by considering the eigenvalues in the plasma frame, in which $\mathbf{u} = 0$. In this case the appropriate eigenvalues simplify to

$$\lim_{u_x \to 0} \lambda_{5,6} = \pm \frac{1}{\sqrt{2}} \sqrt{\gamma_A^2 \left(V_A^2 + \bar{a}^2\right) - \sqrt{\gamma_A^4 \left(V_A^2 + \bar{a}^2\right)^2 - 4\gamma_A^2 a^2 V_{A,x}^2}}, \tag{55}$$

$$\lim_{u_x \to 0} \lambda_{7,8} = \pm \frac{1}{\sqrt{2}} \sqrt{\gamma_A^2 \left(V_A^2 + \bar{a}^2\right) + \sqrt{\gamma_A^4 \left(V_A^2 + \bar{a}^2\right)^2 - 4\gamma_A^2 a^2 V_{A,x}^2}}, \tag{56}$$

where

$$\bar{a}^2 = a^2 \left(1 + \frac{V_{A,x}^2}{c^2}\right). \tag{57}$$

These expressions clearly indicate that λ_5 and λ_6 represent the slow magnetosonic waves, while λ_7 and λ_8 describe the fast ones. We note that these simplified wave speeds are the same as the ones published by Boris [2].

Perpendicular magnetic field. Another interesting special case is when the magnetic field is perpendicular to the x direction, i.e., $V_{\mathrm{A},x} = 0$ and $b_x = 0$, and the slow and the fast wave speeds become

$$\lim_{b_x \to 0} \lambda_{5,6} = u_x, \tag{58}$$

$$\lim_{b_x \to 0} \lambda_{7,8} = \gamma_{\mathrm{A}}^2 u_x \pm \gamma_{\mathrm{A}} \sqrt{a^2 + V_{\mathrm{A}}^2 \left(1 - \gamma_{\mathrm{A}}^2 \frac{u_x^2}{c^2}\right)}. \tag{59}$$

Parallel magnetic field. The opposite limiting case is when the magnetic field is parallel to the x direction, i.e., $b_x = 1$ and $b_y = b_z = 0$. In this case the characteristic wave speeds become,

$$\lim_{b_x \to 1} \lambda_{5,6} = u_x \pm a, \tag{60}$$

$$\lim_{b_x \to 1} \lambda_{7,8} = \gamma_{\mathrm{A}}^2 u_x \pm \gamma_{\mathrm{A}} V_{\mathrm{A}} \sqrt{1 - \gamma_{\mathrm{A}}^2 \frac{u_x^2}{c^2}}. \tag{61}$$

Infinite classical Alfvén speed. A very important limiting case is when the "classical" Alfvén speed approaches infinity, $V_{\mathrm{A}} \to \infty$, and the fast and slow magnetosonic speeds approach

$$\lim_{V_{\mathrm{A}} \to \infty} \lambda_{5,6} = u_x \pm a b_x, \tag{62}$$

$$\lim_{V_{\mathrm{A}} \to \infty} \lambda_{7,8} = \pm c. \tag{63}$$

This is a physically very interesting result. It is obvious that the fast magnetosonic speed is limited by the speed of light in any frame of reference. The slow speed is limited by $u + a$.

Small classical Alfvén speed. Next we return to the P_4 polynomial (46). We note that the second bracketed term is multiplied by V_{A}^2/c^2, a quantity that is small in the nonrelativistic Alfvén speed limit. Neglecting the term proportional to V_{A}^2/c^2 we recover the characteristic polynomial of the nonrelativistic magnetosonic speeds,

$$P_4 = (\lambda - u_x)^4 - \left(V_{\mathrm{A}}^2 + a^2\right)(\lambda - u_x)^2 + a^2 V_{\mathrm{A},x}^2, \tag{64}$$

which has the well-known roots

$$\lim_{V_{\mathrm{A}} \ll c} \lambda_{5,6} = u_x \pm \frac{1}{\sqrt{2}} \sqrt{\left(a^2 + V_{\mathrm{A}}^2\right) - \sqrt{\left(a^2 + V_{\mathrm{A}}^2\right)^2 - 4a^2 V_{\mathrm{A},x}^2}}, \tag{65}$$

$$\lim_{V_{\mathrm{A}} \ll c} \lambda_{7,8} = u_x \pm \frac{1}{\sqrt{2}} \sqrt{\left(a^2 + V_{\mathrm{A}}^2\right) + \sqrt{\left(a^2 + V_{\mathrm{A}}^2\right)^2 - 4a^2 V_{\mathrm{A},x}^2}}. \tag{66}$$

3.3.2. *Approximate Magnetosonic Speeds*

Since quartic equations have analytic solutions, it is possible to obtain closed formulas for the slow and fast magnetosonic speeds. However, these formulas are quite complicated and it is more practical to find the roots of the P_4 polynomial numerically. Here we explore an appoximate solution that is generally valid within a few percent.

A proposed approximate solution of the $P_4 = 0$ equation is given by the slow and fast magnetosonic wave speeds

$$\lambda_{5,6} \approx u_x \pm \bar{c}_s = u_x \pm \frac{1}{\sqrt{2}}\sqrt{\gamma_A^2(\bar{a}^2 + \bar{V}_A^2) - \sqrt{\gamma_A^4(\bar{a}^2 + \bar{V}_A^2)^2 - 4\gamma_A^2 a^2 \bar{V}_{A,x}^2}}, \tag{67}$$

$$\lambda_{7,8} \approx \gamma_A^2 u_x \pm \bar{c}_f = \gamma_A^2 u_x \pm \frac{1}{\sqrt{2}}\sqrt{\gamma_A^2(\bar{a}^2 + \bar{V}_A^2) + \sqrt{\gamma_A^4(\bar{a}^2 + \bar{V}_A^2)^2 - 4\gamma_A^2 a^2 \bar{V}_{A,x}^2}}, \tag{68}$$

where $\bar{c}_s$ and $\bar{c}_f$ are the modified slow and fast magnetosonic speeds, $\bar{a}$ is defined in (57), and we introduce

$$\bar{V}_A^2 = V_A^2\left(1 - \gamma_A^2 \frac{u_x^2}{c^2}\right), \tag{69}$$

$$\bar{V}_{A,x}^2 = V_{A,x}^2\left(1 - \gamma_A^2 \frac{u_x^2}{c^2}\right). \tag{70}$$

It is interesting to note that the slow mode $\lambda_{5,6}$ eigenvalues are symmetric around u_x, while the fast mode $\lambda_{7,8}$ are symmetric with respect to $\gamma_A^2 u_x$. In extreme cases, when u_x is the same order as c, one of the "slow" waves can actually move faster in the laboratory frame than the "fast" wave.

Expressions (67) and (68) have all the right limits. When $u_x \to 0$ they simplify to (55) and (56), and for $b_x \to 0$ they simplify to (58) and (59). In the $b_x \to 1$ limit $a^2 = \gamma_A^2 \bar{a}^2$ and therefore expressions (67) and (68) simplify to (60) and (61). In the relativistic Alfvén speed limit $\gamma_A^2 \to 0$, but $\gamma_A^2 \bar{V}_A^2 \to c^2$ and $\gamma_A^2 \bar{a}^2 \to a^2 b_x^2$, and we recover (62) and (63). In the classical MHD limit $c \to \infty$, $\gamma_A \to 1$, $\bar{V}_A \to V_A$, $\bar{V}_{A,x} \to V_{A,x}$, and $\bar{a} \to a$; thus we obtain (65) and (66). We conclude that expressions (67) and (68) represent a good approximation to the semirelativistic slow and fast magnetosonic wave speeds.

To have a better feeling for the accuracy of the proposed approximate solution we calculate the difference between the P_4 polynomial and the approximate polynomial corresponding to the approximate solutions (67) and (68):

$$\begin{aligned}\bar{P}_4 &= P_4 - (\lambda - u_x - \bar{c}_s)(\lambda - u_x + \bar{c}_s)(\lambda - \gamma_A^2 u_x - \bar{c}_f)(\lambda - \gamma_A^2 u_x + \bar{c}_f) \\ &= \gamma_A^2 \frac{V_A^2}{c^2} 2u_x(\bar{c}_s^2 - a^2 b_x^2)\left[\lambda - \frac{1}{2}u_x(1 + \gamma_A^2)\right].\end{aligned} \tag{71}$$

In general, this residual is quite small because $\bar{c}_s^2 \approx a^2 b_x^2$ is a reasonably good approximation.

Numerical experiments were carried out to check the accuracy of expressions (67) and (68). It was found that these expressions are accurate to within about 2% for the parameter range $0 < a < c/3$, $0 < u_x < c/3$, and $0 < V_A < 3c$. In the parameter range $c/3 < a < c$, $c/3 < u_x < c$, and $0 < V_A < 3c$ (where the nonrelativistic hydrodynamics is no longer applicable) the approximation is still valid to within ~15%.

4. STABILITY

In this section we examine the linear stability for the semirelativistic MHD equations. The equations are linearly stable if the wave speeds are all real. We check this condition for two cases: for a reduced speed of light $c \ll c_0$ and for a true speed of light $c = c_0$.

4.1. Stability with Lowered Speed of Light

From inspection of the modified Alfvén wave speed (48), it is not at all clear that the expression

$$D = \gamma_{\rm A}^2\left(V_{{\rm A},x}^2 - u_x^2\right) + \gamma_{\rm A}^4(u_x + v_{E,x})^2 \tag{72}$$

under the square root is always positive. Indeed, if $D < 0$, one of the Alfvén modes becomes unstable, and its amplitude will grow exponentially. This means that the semirelativistic MHD equations can become unstable. Let us investigate the stability criteria.

First (72) is multiplied by $\gamma_{\rm A}^{-4}$, and $\gamma_{\rm A}$ and $v_{{\rm E},x}$ are substituted from (15) and (49) to yield

$$D_1 = D\gamma_{\rm A}^{-4} = \left(1 + \frac{V_{\rm A}^2}{c^2}\right)\left(V_{\rm A}^2 b_x^2 - u_x^2\right) + \left(u_x + \frac{V_{\rm A}^2}{2c^2}u_{\perp,x}\right)^2. \tag{73}$$

We can now expand inside the parentheses and multiply by the positive $c^2/V_{\rm A}^2$ to obtain

$$D_2 = D\gamma_{\rm A}^{-4}\frac{c^2}{V_{\rm A}^2} = c^2 b_x^2 + V_{\rm A}^2 b_x^2 - u_x^2 + u_x u_{\perp,x} + \frac{V_{\rm A}^2}{4c^2}u_{\perp,x}^2. \tag{74}$$

If we choose a coordinate system in which $B_z = 0$ then

$$u_{\perp,x} = (\mathbf{u}\times\mathbf{b})_z b_y = u b_y \sin\delta, \tag{75}$$

where δ is the angle between the velocity and magnetic field vectors in the x–y plane. We can take $u_z = 0$ since it does not occur in the equations. We introduce the angle α between the x direction and $\mathbf{u}$ and the angle β between the x direction and $\mathbf{b}$, so that $u_x = u\cos\alpha$, $b_x = \cos\beta$, $b_y = \sin\beta$, and $\delta = \alpha - \beta$, Now (74) can be rewritten as

$$D_2 = \left(c^2 + V_{\rm A}^2\right)\cos^2\beta - u^2\left[\cos^2\alpha + \cos\alpha\sin\beta\sin(\alpha-\beta) - \frac{V_{\rm A}^2}{4c^2}\sin^2\beta\sin^2\delta\right]. \tag{76}$$

This expression can be further transformed by expanding the $\sin(\alpha-\beta)$ term to give

$$D_2 = \left(c^2 + V_{\rm A}^2 - u^2\cos^2\alpha\right)\cos^2\beta + \frac{u^2}{4}\left(\frac{V_{\rm A}^2}{c^2}\sin^2\delta\sin^2\beta - \sin 2\alpha\sin 2\beta\right). \tag{77}$$

If $V_{\rm A}/c$ is large then the coefficient of $V_{\rm A}^2/c^2$ must be small at the minimum of D_2; i.e., δ and/or β must be small. In either case it can be easily shown that D_2 remains positive as long as

$$u^2 < c^2 + V_{\rm A}^2. \tag{78}$$

This condition is easy to meet: one should simply make sure that the artificially lowered c remains above the maximum of $|\mathbf{u}|$.

Now we return to the more challenging small $\boldsymbol{V}_{\rm A}/c$ case. We minimize (77) in terms of β, with the approximation that $\alpha = \delta - \beta$ is independent of β. This approximation will turn out to be very reasonable. The minimum of D_2 is at

$$\tan 2\beta_{\min} = -\frac{(u^2/2)\sin 2\alpha}{c^2 + V_{\rm A}^2 - u^2\cos^2\alpha - \left(V_{\rm A}^2 u^2/4c^2\right)\sin^2\delta}, \tag{79}$$

where we should take the solution at

$$\beta_{\min} \approx \frac{\pi}{2} - \frac{u^2}{4c^2} \sin 2\alpha. \tag{80}$$

Here we assumed that both V_A and u are much less than c, thus the denominator of (79) is dominated by the very first term c^2, and $\tan 2\beta \approx 2\beta - \pi$. (The $\tan 2\beta \approx 2\beta$ solution yields the maximum for D_2). Clearly, $\beta_{\min}$ must be very close to $\pi/2$, so we can take $\alpha = \delta + \pi/2$, $\sin\beta \approx 1$, and $\cos\beta \approx (u^2/4c^2)\sin 2\delta$. Substituting all this back into (77) results in

$$\min D_2 \approx \frac{u^2}{4c^2} \sin^2\delta \left(V_A^2 - u^2\cos^2\delta\right) = \frac{u_\perp^2}{4c^2}\left(V_A^2 - u_\parallel^2\right) \tag{81}$$

which is positive if

$$u_\parallel < V_A \tag{82}$$

Interestingly, this stability condition does not depend on c, i.e., any flow that has a speed parallel to the magnetic field exceeding the nonrelativistic Alfvén speed is unstable in the semirelativistic approximation if $V_A \ll c$. This looks like a contradiction to the well known fact that the nonrelativistic Alfvén speed is always real, which we should obtain as the $c \to \infty$ limit of the semirelativistic solution. The explanation is the following: in the $c \to \infty$ limit both the nonrelativistic and semirelativistic Alfvén speeds approach zero for the propagation direction at an angle $\beta \to \pi/2$ with the magnetic field. The nonrelativistic solution, however, converges to 0 on the real axis, while the semirelativistic solution converges to 0 on the complex plane with a small imaginary part. We can actually calculate the real and imaginary parts of the most unstable Alfvén mode in the $V_A < u_\parallel \ll c$ limit:

$$\Re(\lambda_{3,4}) \approx u_\perp \tag{83}$$

$$\Im(\lambda_{3,4}) \approx \pm\frac{u_\perp V_A}{2c^2}\sqrt{u_\parallel^2 - V_A^2}. \tag{84}$$

The imaginary part is clearly quite small and it is always smaller than the real part.

We have explored numerically the parameter range in which V_A is the same order as c. Figure 1 shows the numerically obtained maximum stable field-aligned flow speed $u_{\parallel,\max}$ as a function of the Alfvén speed $0 < V_A/c < 1$ and the angle $0 < \delta < 90°$. The approximation $u_{\parallel,\max} \approx V_A$ from (82) is a lower bound to the numerically obtained values. It is an extremely good approximation in the lower left part of the figure, where the contour lines are vertical. Where the contour lines bend to the left, $u_{\parallel,\max} > V_A$, while in the upper right black triangular area $u_{\parallel,\max} = \infty$; i.e., the equations are stable for any $u_\parallel$.

We conclude that the near conservation form of the semirelativistic MHD equations are only conditionally stable when the speed of light is artificially lowered. In the large and small Alfvén speed limits sufficient stability criteria are given by (78) and (82). The acceleration technique should be applied when V_A is large, so that the magnetosonic and Alfvén speeds are reduced by the artificial lowering of the speed of light. In this limit the equations are stable as long as $u < c$. In fact, there is not much point in lowering c below u, since eventually the time step will become limited by the slow wave, which propagates at speed $u \pm a$ parallel to the field lines according to (62).

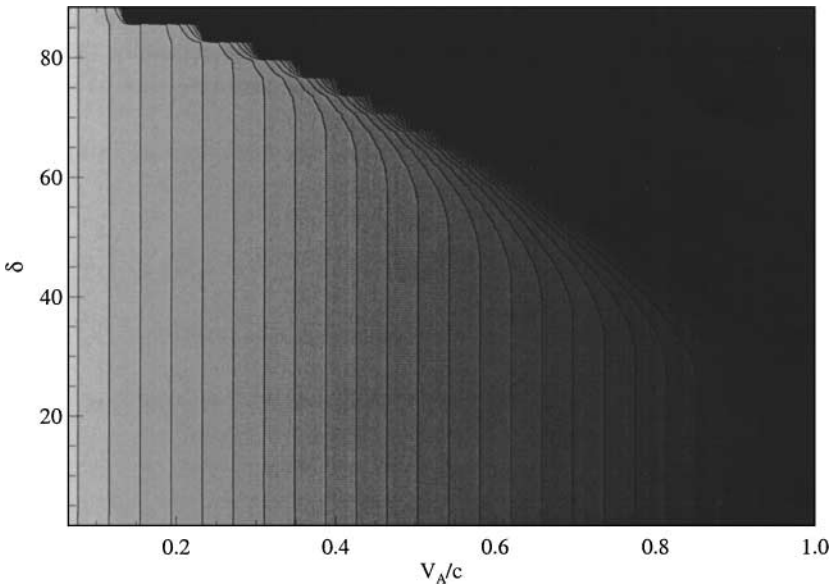

FIG. 1. The maximum parallel velocity $u_{\parallel,\max}$ as a function of the non-relativistic Alfvén speed V_A and the angle between the velocity and magnetic field vectors δ (in degrees). The approximate formula $u_{\parallel,\max} = V_A$ is almost exact where the contour lines are straight. In the upper right region $u_{\parallel,\max} = \infty$, i.e., the solution is stable for any value of $u_\parallel$.

Difficulties arise only if in some parts of the computational domain the Alfvén speed is large ($V_A > c$), while in other parts it is small ($V_A \ll c$) and the field-aligned flow can become super-Alfvénic ($u_\parallel > V_A$). Even under these circumstances it is possible that the numerical solution remains stable, because the weak instability might be suppressed by the numerical diffusion of the scheme. In any case, one can always switch to the nonrelativistic MHD equations in parts of the computational domain where V_A is small, and where the acceleration technique does not have much use anyway. This hybrid approach should still yield correct steady-state solutions.

Finally, we note that the approximate formulas (67) and (68) for the slow and fast waves always yield real wave speeds as long as $1 - \gamma_A^2 u_x^2/c^2 > 0$ in (69) and (70), which gives the same condition as (78). This can be easily shown by substituting Eq. (57) into the expressions under the inner square roots of (67) and (68).

4.2. Stability without Lowering the Speed of Light

Although we could not solve the eigenvalue problem in its full generality for the $c = c_0$ case, i. e., when there is no artificial lowering of the speed of light and the source term $\mathbf{Q} = 0$, our partial analytic and numerical results suggest that in this case all eigenvalues are real as long as $u < c$. In other words, the semirelativistic MHD equations *with the true value of the speed to light* are stable for $u < c$. We have proved this rigorously for the case when the unperturbed vectors $\mathbf{B}$ and $\mathbf{u}$ and the x axis are coplanar. In this case we may choose a coordinate system in which $B_z = u_z = 0$. The fast and slow wave speeds are then the same as above, because these waves do not produce B_z and u_z; thus $E_x = 0$, which means that the source term $\mathbf{Q} \propto \nabla \cdot \mathbf{E} = 0$ does not play any role. The Alfvén waves, on the other hand,

have new eigenvalues

$$\lambda'_{3,4} = u_x - v_{s,x} \pm \sqrt{\gamma_A^2 V_{A,x}^2 \left(1 - \frac{u^2}{c^2}\right) + v_{s,x}^2}, \tag{85}$$

where

$$\mathbf{v}_s = \gamma_A^2 \frac{V_A^2}{c^2} u_\parallel \mathbf{b}. \tag{86}$$

Clearly, the eigenvalues $\lambda'_{3,4}$ are real as long as $u < c$.

5. WAVE SPEEDS AND STABILITY OF THE SIMPLIFIED EQUATIONS

In this section we examine the eigenvalues and the stability of the two simplified approximations to the semirelativistic MHD equations, which were discussed in Section 2.8.

5.1. The Boris simplification

In this case the entropy and $\nabla \cdot \mathbf{B}$ wave speeds remain unchanged ($\lambda_{1,2} = u_x$). The Alfvén waves propagate with speeds given by

$$\lambda^s_{3,4} = \frac{1}{2}\left[\left(1 + \gamma_A^2\right)u_x \pm \sqrt{\left(1 - \gamma_A^2\right)^2 u_x^2 + 4\gamma_A^2 V_{A,x}^2}\right]. \tag{87}$$

We note that these wave speeds are not symmetric with respect to the flow speed. This effect is due to the inclusion of the Poynting vector in the conserved momentum and has already been discussed. The expression under the square root is always positive, since it is the sum of two squares, which implies that the Alfvén waves are stable in this case. In the limit of $V_A \gg c$ it can be shown that $|\lambda^s_{3,4}| < |u_x| + c$.

The magnetosonic wave speeds can only be expressed by very long and complicated formulas and in practice they can be obtained by numerically solving the roots of a fourth-order polynomial. For the special case of $\mathbf{u} = 0$, i.e., in the plasma frame, the wave speeds are

$$c^s_{\text{fast,slow}} = \frac{\gamma_A}{\sqrt{2}} \sqrt{a^2 + V_A^2 \pm \sqrt{\left(a^2 + V_A^2\right)^2 - 4a^2 V_{A,x}^2}}, \tag{88}$$

which are simply the classical magnetosonic speeds multiplied by γ_A; thus, at least in the plasma frame, the magnetosonic waves of the simplified equations are always stable. The fast speed is limited by c for $V_A \gg c$, since $\gamma_A V_A \to c$ as $V_A \to \infty$. For the numerical schemes we need an approximate formula for the maximum propagation speed. We adopt $|u_x| + c^S_{\text{fast}}$ as a good upper estimate.

We note that Boris [2] published wave speeds for the unsimplified semirelativistic equations in the plasma frame; these are different from the wave speeds of the simplified equations discussed here.

5.2. Reduced j × B Force

In this case the entropy and $\nabla \cdot \mathbf{B}$ wave speeds again remain unchanged ($\lambda_{1,2} = u_x$). The Alfvén and magnetosonic waves propagate with speeds given by

$$\lambda^{\mathrm{R}}_{3,4} = u_x \pm \gamma_{\mathrm{A}} V_{\mathrm{A},x}, \tag{89}$$

$$\lambda^{\mathrm{R}}_{5,6,7,8} = u_x \pm \frac{1}{\sqrt{2}} \sqrt{a^2 + \gamma_{\mathrm{A}}^2 V_{\mathrm{A}}^2 \pm \sqrt{\left(a^2 + \gamma_{\mathrm{A}}^2 V_{\mathrm{A}}^2\right)^2 - 4a^2 \gamma_{\mathrm{A}}^2 V_{\mathrm{A}}^2}}, x. \tag{90}$$

All the wave speeds are guaranteed to be real, since $V_{\mathrm{A},x} \le V_{\mathrm{A}}$. In the $V_{\mathrm{A}} \to \infty$ limit the fast speeds are $u \pm \sqrt{a^2 + c^2}$ perpendicular to the magnetic field.

We conclude that both simplified approximations lead to stable equations, and the Boris simplification also preserves the steady-state solution of nonrelativistic MHD.

6. SPLITTING THE MAGNETIC FIELD

For problems in which strong externally imposed magnetic fields are present, accuracy can be increased by solving for the deviation of the magnetic field from this prescribed component. For instance, in magnetosphere-type simulations a strong dipole-like magnetic field dominates the solution near the body. Solving for the deviation $\mathbf{B}_1$ from the embedded field $\mathbf{B}_0$ is inherently more accurate than solving for the full magnetic field vector $\mathbf{B} = \mathbf{B}_0 + \mathrm{B}_1$. This approach was first suggested by Ogino and Walker [15], applied to Godunov-type schemes by Tanaka [20], and later employed by our group [17]. Here we generalize it to semirelativistic MHD.

The full magnetic field vector $\mathbf{B}$ can be written as

$$\mathbf{B} = \mathbf{B}_0 + \mathbf{B}_1, \tag{91}$$

where $\mathbf{B}_0$ is given analytically and thus $\nabla \cdot \mathbf{B}_0 = 0$, while $\mathbf{B}_1$ is calculated by the numerical scheme. Note that $\mathbf{B}_1$ is not necessarily small relative to $\mathbf{B}_0$. We also introduce the nonrelativistic current density $\mathbf{j}_0 = (1/\mu_0)\nabla \times \mathbf{B}_0$. The splitting is most important when the equations are solved in a (near) conservation form, since the total density $\varepsilon + e_{\mathrm{A}}$ can be completely dominated by the magnetic energy $\mathbf{B}_0^2/(2\mu_0)$. When the pressure is calculated from the total energy density, it can easily become negative, as we take difference of two huge numbers to obtain a small one. This problem can be mitigated by rewriting the energy equation in terms of the modified total energy density

$$e_1 = \varepsilon + \frac{1}{2\mu_0}\left(B_1^2 + \frac{1}{c^2}E^2\right). \tag{92}$$

Note that the electric energy still contains contribution from $\mathbf{B}_0$, but that is reduced by the factor $(1/c^2)$. With these definitions the near conservation form of the semirelativistic MHD equations (27) can be rewritten as

$$\frac{\partial}{\partial t}\rho + \nabla \cdot (\rho \mathbf{u}) = 0, \tag{93}$$

$$\frac{\partial}{\partial t}\left(\rho \mathbf{u} + \frac{1}{c^2}\mathbf{S}_{\mathrm{A}}\right) + \nabla \cdot [\rho \mathbf{u}\mathbf{u} + \mathbf{I}p + \mathbf{P}_{\mathrm{A},1}] = \mathbf{Q} + \mathbf{j}_0 \times \mathbf{B}_0, \tag{94}$$

$$\frac{\partial}{\partial t}\mathbf{B}_1 + \nabla \cdot [\mathbf{uB} - \mathbf{Bu}] = \frac{\partial \mathbf{B}_0}{\partial t}, \tag{95}$$

$$\frac{\partial}{\partial t}e_1 + \nabla \cdot \left[\mathbf{u}\left(\frac{1}{2}\rho \mathbf{u}^2 + \frac{\gamma p}{\gamma - 1}\right) + \frac{1}{\mu_0}\mathbf{E} \times \mathbf{B}_1\right] = -\mathbf{B}_1 \cdot \frac{\partial \mathbf{B}_0}{\partial t} + \mathbf{E} \cdot \mathbf{j}_0, \tag{96}$$

where

$$P_{\mathrm{A},1} = \frac{1}{\mu_0}\left[\mathbf{I}\left(\frac{1}{2}\mathbf{B}_1^2 + \mathbf{B}_1 \cdot \mathbf{B}_0 + \frac{1}{2c^2}\mathbf{E}^2\right) - \mathbf{B}_1\mathbf{B}_1 - \mathbf{B}_1\mathbf{B}_0 - \mathbf{B}_0\mathbf{B}_1\right]. \tag{97}$$

The splitting did not modify the continuity equation. In the momentum equation the dominant $B_0^2\mathbf{I}$ and $\mathbf{B}_0\mathbf{B}_0$ terms are moved into the source term $\mathbf{j}_0 \times \mathbf{B}_0$, which can be calculated analytically, and it is identically zero if $\mathbf{B}_0$ is a force-free field. The induction equation is modified in a trivial way, by moving the time derivative of $\mathbf{B}_0$ to the right-hand side. Again, this term can be calculated analytically, and in the case of a stationary $\mathbf{B}_0$ field, it vanishes. The split energy equation is obtained after quite some algebra. Most of the dominant B_0^2 and $\mathbf{E} \times \mathbf{B}_0$ terms are eliminated, but the remaining source terms $\mathbf{B}_1 \cdot \partial \mathbf{B}_0/\partial t$ and $\mathbf{E} \cdot \mathbf{j}_0$ contain the numerically calculated $\mathbf{B}_1$ and $\mathbf{u}$ quantities. In case of a potential ($\mathbf{j}_0 = 0$) and/or stationary $\mathbf{B}_0$ field one or both energy source terms can be eliminated.

One may add the source terms involving $\nabla \cdot \mathbf{B}$ to the split momentum, induction, and/or energy equations (94)–(96) if the numerical scheme does not keep $\nabla \cdot \mathbf{B}$ exactly zero. Of course, $\nabla \cdot \mathbf{B} = \nabla \cdot \mathbf{B}_1$, since the analytic $\mathbf{B}_0$ field must be divergence free by definition.

7. NUMERICAL TESTS

7.1. Implementation

In our code, BATS-R-US [17], the near conservation form (27) of the semirelativistic MHD equations is implemented with the state vector (9), flux diad (10), and source (28). The main steps of the algorithm are;

1. Determine time step Δt based on the approximate wave speeds (67) and (68).
2. Calculate limited slopes of the conservative variables (9).
3. Obtain left and right states at the cell interfaces.
4. Transform interface states to primitive variables (16).
5. Calculate physical fluxes at cell interfaces (10).
6. Add numerical fluxes based on the wave speeds (67) and (68).
7. Calculate source terms at cell centers (28).
8. Add fluxes and sources to the conservative variables at cell centers.

The only nontrivial modification of an existing nonrelativistic MHD code to the semirelativistic equations involves the modification of the numerical fluxes. Currently the semirelativistic MHD equations are discretized with the second-order Rusanov (TVD Lax–Friedrichs) and the second-order HLL Linde [12] schemes in BATS-R-US. These schemes only require the maximum propagation speed (68). Applying the Roe-type approximate Riemann solver poses a more difficult problem, because it requires the eigenvectors of the characteristic matrix (42), which are very complicated expressions. We note that the evaluation of the source term in (28) requires the use of slope limiters to obtain $\nabla \cdot \mathbf{E}$, which shows that this term can be very important.

In certain simulations it is difficult to maintain positivity of pressure, because it is calculated from the total energy density $\varepsilon + e_A$ which can be dominated by the kinetic and electromagnetic terms. Even a relatively small truncation error may lead to a negative pressure. There are several ways to improve the situation. First, we calculate pressure rather than total energy at the cell interfaces; thus the limited slopes are applied on pressure. This ensures that the cell-interface pressure is always positive. Second, we have the option of updating p with the nonconservative equation (20) in certain parts of the computational domain. Using the conservative energy equation is only important for obtaining correct jump conditions across shock waves. One can use some dynamic switch [1] to identify shock waves, or in some problems one can use simple geometrical conditions to select the appropriate energy equation.

In all time-accurate tests, a spatially and temporally second-order high-resolution MUSCL type TVD scheme is used with a Lax–Friedrichs flux function and a monotonized central (Woodward) limiter (see [22] for a detailed description). The 8-wave scheme is used to control the numerical error in $\nabla \cdot \mathbf{B}$ in the multidimensional simulations. In one-dimensional simulations $\nabla \cdot \mathbf{B} = 0$ is automatically satisfied. The explicit time steps are limited by the Courant–Friedrich–Lewy (CFL) stability condition. The maximum Courant number is set to $C = 0.9$. We use SI units; thus the true speed of light is $c_0 = 3 \times 10^8$ m/s.

7.2. Propagation of Alfvén Waves

Our first numerical test involves the propagation of Alfvén waves. The intial condition is $\rho = 1$, $u_x = 0.5$, $u_y = 0$, $p = 0.1$, $B_x = B_y = 1$, and $B_z = 0$, with $u_z = 0.01$ for $x < 0$ and $u_z = -0.01$ for $x > 0$. The adiabatic index is $\gamma = 2$ and the magnetic units are normalized such that $\mu_0 = 1$. The reduced speed of light is set to $c = 0.9$, which is below the Alfvén speed $V_A = \sqrt{2}$ but is above the flow speed $u = 0.5$. The $-400 < x < 400$ domain is resolved with 800 grid cells.

Figure 2 shows the solution at time $t = 200$. The left- and right-propagating Alfvén waves are at $x \approx -57.4$ and 150.6 in perfect agreement with the analytic predictions based on (48). These values should be compared with locations of the nonrelativistic Alfvén waves, which would propagate at speeds $u_x \pm V_{A,x} = 0.5 \pm 1$, so they would be at $x = -100$ and 300 at time $t = 200$. The semirelativistic approximation reduced the Alfvén speed below c in an asymmetric fashion. The locations of the left- and right-going waves are symmetric around $\gamma_A^2(u_x + v_E)t \approx 46.6$ rather than the nonrelativistic $u_x t = 100$. Also note that the original discontinuity in u_z was symmetric around 0, but the two waves carry different jumps in u_z. This asymmetry is also due to the non-Galilean invariance of the semirelativistic equations.

Table I presents numerical values of the left- and right-running Alfvén speeds for the one-dimensional numerical test discussed in this Section. The four columns represent Alfvén speeds calculated using the full semirelativistic MHD equations (Eq. (48)), the simplified

TABLE I
Comparison of Alfvén Speeds

Wave	Semirelativistic MHD	Simplified	Reduced $\mathbf{j} \times \mathbf{B}$	Nonrelativistic MHD
Left	−0.2869	−0.2434	−0.0366	−0.5
Right	+0.7529	+0.8874	+1.0366	+1.5

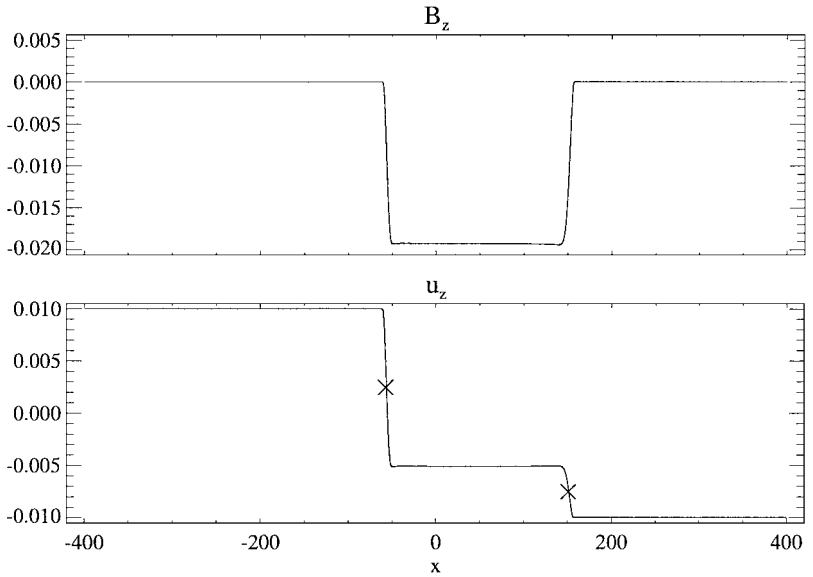

FIG. 2. The z components of velocity and magnetic field in the Alfvén wave propagation test at time $t = 200$. The $\times$ symbols show where the waves are expected to be based on the analytic formula (48).

set of equations given by Eqs. (38) and (39) (the solution is given by (87), the reduced $\mathbf{j} \times \mathbf{B}$ approximation given by Eq. (89), and the nonrelativistic speeds $u_x \pm V_{\mathrm{A},x}$, respectively.

7.3. Unstable Alfvén Modes

We also simulated an unstable Alfvén mode based on the discussion in Section 4.1. The initial condition is $\rho = 1$, $u_x = 0.6453$, $u_y = -0.4728$, $p = 0.1$, $B_x = 0.076256$, $B_y = -0.49415$, and $B_z = 0$, with $u_z = 0.01$ for $x < 0$ and $u_z = -0.01$ for $x > 0$. The other parameters $c = 0.9$, $\gamma = 2$, $\mu_0 = 1$, and the grid are the same as in the previous test.

The initial condition was carefully chosen to produce an unstable mode. The bulk speed and the nonrelativistic Alfvén speeds are $u = 0.8$ and $V_{\mathrm{A}} = 0.5$. The angle between the velocity and magnetic field vectors is $\delta = 45^\circ$; thus $u_\parallel > V_{\mathrm{A}}$. The magnetic field is at an angle $\beta = -81.2^\circ$ relative to the x direction, which is close to the most unstable angle. With these parameter choices, the complex eigenvalues of the semirelativistic Alfvén modes are $\lambda_{3,4} = 0.572 \pm i0.0336$ from (48).

Figure 3 shows a time series of the solution. The first leftmost curves at $x \approx 10$ correspond to $t = 20$ while the final rightmost curves are located at $x \approx 110$ at $t = 200$. The distance between them agrees well with $(200 - 20)\Re(\lambda) \approx 100$. The wavelength of the fastest growing mode is around 20 units, which corresponds to a wave number $k = 2\pi/20 \approx 0.31$. The dashed line in the lower panel of the figure shows the theoretical growth of

$$\min_x u_z(t) = u_{z,0} e^{k\Im(\lambda_3)t} = -0.01 e^{0.0182x}, \tag{98}$$

where we used $t = x/\Re(\lambda)$ to convert the position of the peak to time. The agreement with the numerical results is excellent.

We note that the growth of modes with shorter wavelengths is suppressed by numerical dissipation. If the gird resolution is increased the wavelength of the fastest growing mode

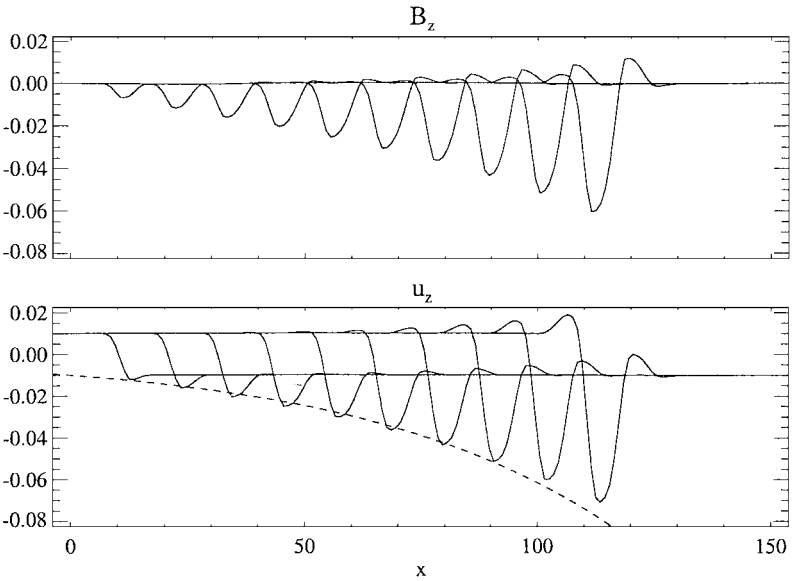

FIG. 3. The z components of the velocity and the magnetic field in the unstable Alfvén wave propagation test. The solution are overplotted for times $t = 20, 40, \ldots, 200$. The wave is propagating to the right. The dashed line in the lower panel shows the theoretical growth (98) of the velocity peak.

becomes shorter and the growth rate becomes larger. As the amplitude of the mode becomes nonlinear, however, the growth tends to slow down. It was also checked numerically that without the **Q** source term, i.e., if $c = c_0 = 0.9$, the Alfvén mode is stable, as we expect from (85).

7.4. Propagation of Fast and Slow Waves

This numerical test involves the propagation of slow and fast waves. The initial condition is $\rho = 1$, $u_y = u_z = 0$, $p = 0.1$, $B_x = B_y = 1$, and $B_z = 0$, with $u_x = 0.51$ for $x < 0$ and $u_x = 0.49$ for $x > 0$. Again $\gamma = 2$, $\mu_0 = 1$, and the reduced speed of light is $c = 0.9 < v_A = \sqrt{2}$. The grid is the same as in the Alfvén wave propagation test.

The small jump in u_x results in four magnetosonic waves, as shown in Fig. 4. The numerically obtained locations of the waves are in excellent agreement with analytic predictions calculated from the roots of the characteristic equation (46). The analytic values for the locations of the left- and right-propagating fast waves are $x \approx -120.4$ and 182.9, while the slow waves are at $x \approx 38.4$ and 156.6. Even the approximate values provided by (67) and (68) agree within a few percent, even though the parameters are rather extreme, e.g., $u \approx 0.55c$ and $a = \sqrt{0.2} \approx 0.5c$. These values should be compared with locations of the nonrelativistic fast waves, which would be at $x = -190.2$ and 390.4 at the same time. Again, the semirelativistic approximation reduced the magnetosonic speeds below c. The fast waves are positioned symmetrically with respect to $\gamma_A^2 u_x t = 28.8$, while the slow waves are symmetric around $u_x t = 100$. The original discontinuity in u_x was symmetric around 0.5, but the four waves split this discontinuity in an asymmetric fashion.

Table II presents numerical values of the left- and right-running slow and fast waves for the one-dimensional numerical test discussed in this Section. The five columns represent wave speeds calculated using the full semirelativistic MHD equations (numerical roots of

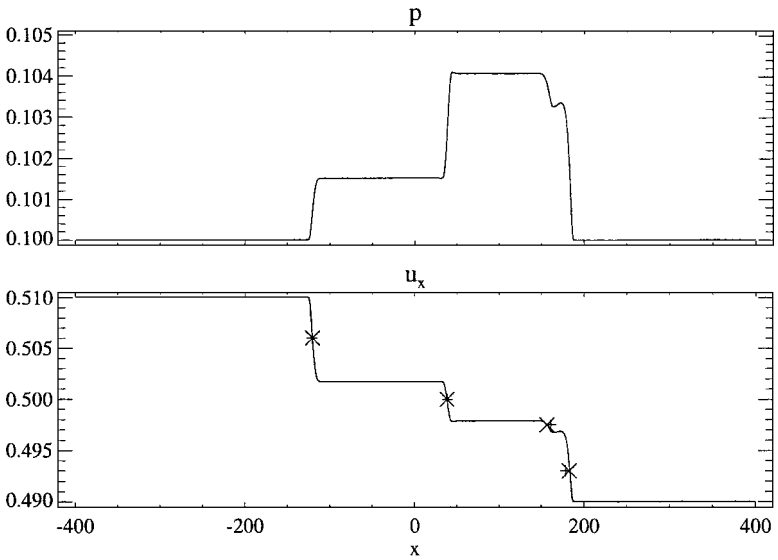

FIG. 4. The pressure and the x component of velocity in the fast and slow wave propagation test at time $t = 200$. The $\times$ symbols show where the waves are expected to be based on the exact roots of the P_4 polynomial in (46), while the $+$ symbols correspond to the approximate formulae (67) and (68).

Eq. 46), the approximate solution given by (67) and (68), the simplified set of equations given by Eq. (38) and (39), the reduced $\mathbf{j} \times \mathbf{B}$ approximation given by Eq. (90), and the nonrelativistic MHD speeds (65) and (66).

7.5. Standing Waves

We carefully checked that a standing Alfvén slow, or fast wave, is a solution of the nonrelativistic as well as the full semirelativistic and Boris's simplified semirelativistic MHD equations. These tests are very similar to the tests presented in the previous sections, with the following modifications: the initial $u_x = \pm V_{\mathrm{A},x}$ in the Alfvén wave test, while the initial u_x is symmetric around $\pm c_{s,x}$ or $\pm c_{f,x}$ in the slow and fast wave test, where $V_{\mathrm{A},x}$, $c_{s,x}$ and $c_{f,x}$ are the nonrelativistic Alfvén, slow, and fast wave speeds, respectively. The tests confirmed that the steady-state solutions are the same (within truncation error) in the nonrelativistic and (simplified) semirelativistic cases.

The reduced $\mathbf{j} \times \mathbf{B}$ approximation does not preserve the steady state of the nonrelativistic MHD equations. The error can be estimated from the difference of the wave speeds in the last two columns of Tables I and II since both the nonrelativistic MHD and the reduced

TABLE II
Comparison of Magnetsosonic Speeds

Wave	Semirelativistic MHD (numerical)	Semirelativistic MHD (approx.)	Simplified Boris	Reduced $\mathbf{j} \times \mathbf{B}$	Nonrelativistic MHD
Fast left	−0.6017	−0.6042	−0.5811	−0.3324	−0.9509
Slow left	+0.1921	+0.1938	+0.0560	+0.2117	+0.1918
Slow right	+0.7831	+0.8062	+0.6066	+0.7883	+0.8082
Fast right	+0.9144	+0.8921	+1.2065	+1.3324	+1.9509

$\mathbf{j} \times \mathbf{B}$ approximations are Galilean invariant. The wave speed differences are 0.47, 0.62, and 0.02 for the Alfvén, fast, and slow waves, respectively.

7.6. Convergence toward Steady State

As a practical application of the acceleration technique, we do a simplified three-dimensional magnetosphere-type run. The simulation domain is $-224R_E < x < 32R_E$, $-64R_E < y, z < 64R_E$, where $R_E = 6378$ km is the radius of Earth. The solar wind enters at the $x = 32R_E$ boundary with a velocity vector $u_x = -400$ km/s, $u_y = u_z = 0$, density $5\, m_p/\text{cm}^3$ (where m_p is the mass of the proton), temperature $T \approx 182{,}000$ K, and an adiabatic index $\gamma = 5/3$. In this simulation the solar wind carries a northward-pointing interplanetary magnetic field with $B_z = 5$ nT, $B_x = B_y = 0$. The outer boundary conditions are very simple: at $x = 32R_E$ there is superfast inflow of the solar wind, and at the other parts of the outer boundary we apply a zero gradient condition.

At the origin there is a solid body with radius $3R_E$, which represents the Earth with its dipole dominated surrounding. We place the inner boundary at $3R_E$ to avoid the extremely strong magnetic field inside this radius. The Earth's dipole strength is charcterized by the magnetic field strength at the equator, which is about 31,100 nT at $1R_E$. For this simplified test the dipole is aligned with the z axis, with its magnetic north pole in the southern ($z < 0$) hemisphere.

The inner boundary condition for the velocity is reflection of all components, which means that there is no normal mass flux and no tangential slipping. The rotation of the Earth is neglected in this test. The density is fixed to the solar wind value of $5\ m_p/\text{cm}^3$ and the temperature to 35,000 K at the inner boundary. The magnetic field is split into the dipole field $\mathbf{B}_0$ and the deviation $\mathbf{B}_1$. The boundary conditions on the deviation field are the following: the radial component $B_{1,r}$ is set to zero, while the tangential components of $\mathbf{B}_1$ have zero gradient across the inner boundary. This boundary condition ensures that the total field has no net magnetic monopole inside the inner boundary, while the tangential components are allowed to produce a current $\nabla \times \mathbf{B}_1$. Typically $\mathbf{B}_1$ is negligible relative to $\mathbf{B}_0$ close to the Earth. Even at $3R_E$ the magnetic field is so strong that the Alfvén speed is around 18,000 km/s for the typical plasma densities. This can severely limit the time step.

The computational domain is resolved with a block-adaptive grid consisting of 1724 blocks. Each Cartesian block contains $4 \times 4 \times 4$ cells, so there are are altogether 110,336 cells. The cell sizes vary between blocks, however. The coarsest blocks have cubic cells with $\Delta x = 8R_E$, while the finest blocks have $\Delta_x = 1R_e$. The finer cells are concentrated around the body and at the expected location of the bow shock and the magnetotail. The initial conditions have the solar wind density, pressure, and velocity everywhere, but initially the magnetic field contains the dipole field only ($\mathbf{B} = \mathbf{B}_0$, $\mathbf{B}_1 = 0$), and the interplanetary field is propagated in from the inflow boundary as the simulation proceeds. Thus the initial magnetic field is divergence free.

The simulations were run with a spatially first-order-accurate Linde scheme [12] for up to 1.5 hours, which allows the interplanetary magnetic field to propagate 5400s $\times$ 400 km/s $\approx 343R_E$, which exceeds the $256R_E$ length of the computational domain. At this point the spatial order is switched to second order using the symmetric β-limiter function (described in [6], p. 543, Eq. 21.3.35), and the simulation is stopped after 6 hour of physical time. By this time the solutions have converged to a steady state, except for some insignificant oscillations.

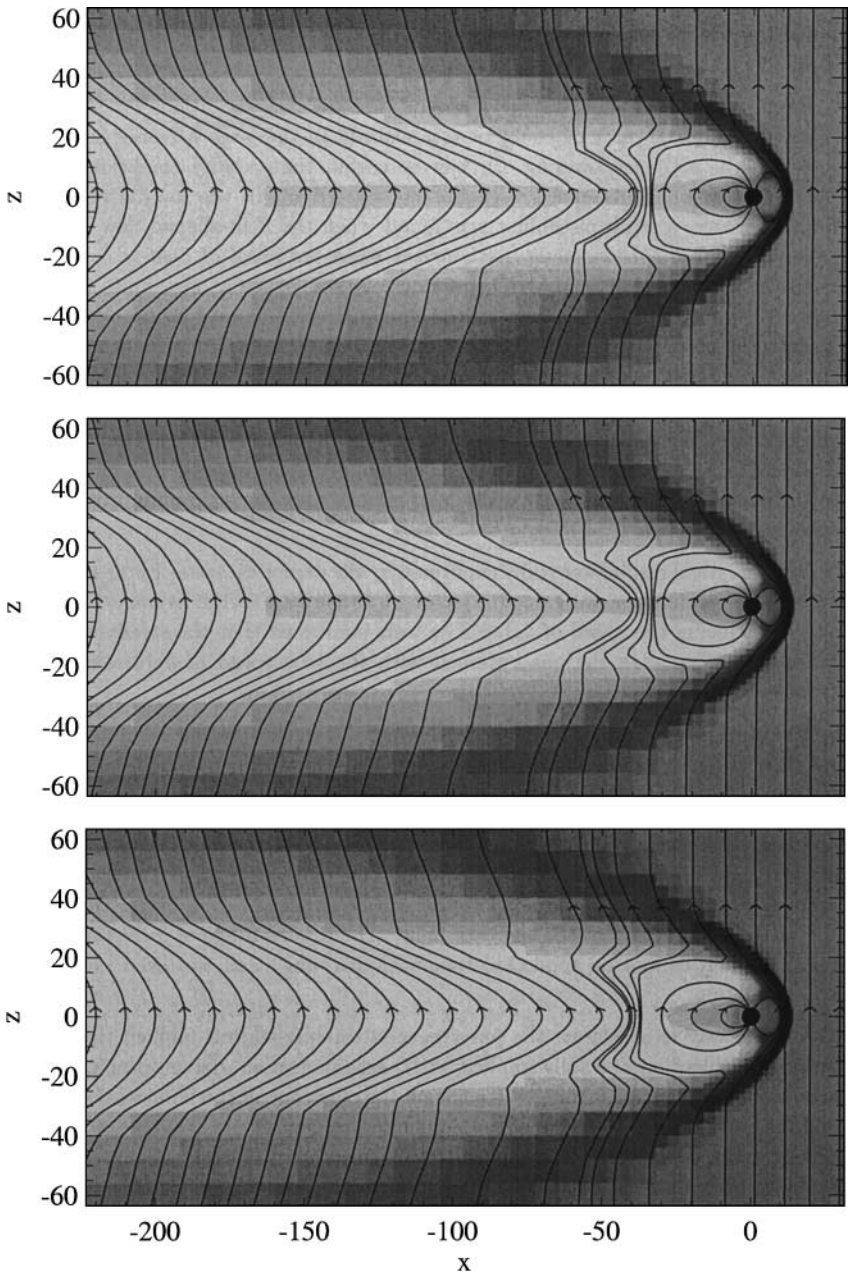

FIG. 5. The steady-state solutions in the $y = 0$ planes of the nonaccelerated run with $c = c_0$ (top panel) and the accelerated runs with $c = c_0/200$ without (middle panel) and with (bottom panel) Boris's simplification. The density (grayscale), the magnetic field (black lines), and the central body (black circle) are shown.

We compare the results of three runs: one with $c = c_0$ and the others with a reduced speed of light $c = c_0/200 \approx 1500$ km/s with and without Boris's simplification. The steady states obtained with the three methods are shown in Fig. 5. Although there are some small differences due to the truncation errors of the rather coarse discretization, the overall results clearly agree very well. The nonaccelerated run requires about 311,000 time steps to reach

$t = 6$ hours, while in the accelerated simulations only about 25,000 time steps were needed. This is a factor of 12.4 gain in CPU time!

8. CONCLUSIONS

We derived the semirelativistic MHD equations as the nonrelativistic hydrodynamic limit of the relativistic MHD equations ($a \ll c$ and $u \ll c$). The same system of equations was obtained from the nonrelativistic MHD equations by keeping the displacement current and charge density, which are usually neglected. These equations are suitable for modeling plasmas where the nonrelativistic Alfvén speed would approach or exceed the speed of light.

The steady-state solution of these equations is independent of the value of the speed of light applied in the displacement current term. By artificially lowering c below the true speed of light c_0 in this term, one can reduce the wave speeds, which allows larger time steps for explicit numerical schemes. When the equations are written in a conservation from, a source term appears when $c \neq c_0$. This term results from our always having to use c_0 in the charge density to obtain a valid steady-state solution.

The wave speeds, which are required by various numerical schemes, were calculated. We have found the exact solutions for all wave speeds, although the fast and slow speeds are roots of a general quartic equation. We have also discovered some very accurate and relatively simple approximations for the slow and fast wave speeds. All the wave speeds are bounded by $c + |u| + a$, unlike in nonrelativistic MHD, in which the Alfvén speed $V_A = B/\sqrt{\mu_0 \rho}$ can be arbitrarily larger than $c + |u| + a$. For the numerical schemes considered in this paper, the wave speeds are used to adjust the numerical fluxes so that they provide stability without excessive dissipation. The approximations in the formulas only have an effect on the numerical dissipation, but the consistency of the discretization is not compromised at all.

Based on the characteristic wave speeds, the stability conditions for the semirelativistic MHD equations can be established. In the high-Alfvén-speed limit, in which the artificial lowering of c can be useful, the stability condition is very unrestrictive: the bulk speed u should not exceed c. In the low-Alfvén-speed limit, however, a weak instability was found when the field-aligned flow speed is super-Alfvénic. *This instability only arises when the speed of light is artificially reduced*; the semirelativistic MHD equations are stable. If this instability becomes a practical problem in some parts of the simulation domain, we propose switching back to the nonrelativistic MHD equations in that region. This will not affect the time-step restriction, since the Alfvén speed is low, and it will not influence the steady-state solution either.

Alternatively, one can also use Boris's simplified equations to obtain a steady-state solution of the nonrelativistic MHD equations. The simplified equations are fully conservative. We calculated the Alfvén wave speed for this simplified equation and found it to be unconditionally stable. The magnetosonic speeds were only found in the plasma frame, but we gave an upper estimate for the maximum propagation speed.

Our analytical results were fully confirmed by the numerical tests. In the magnetosphere-type simulation we gained a factor of about 12.4 in the average time-step size by reducing the speed of light. The tests confirmed that the steady-state solution is the same as the one obtained with the true speed of light, except for truncation-level errors.

There are several other ways to accelerate convergence to steady state. Local time stepping is one of the simplest and most powerful technique and it has been used in the BATS-R-US

code with great success. In the local-time-stepping-algorithm the time step Δt is different for each computational cell, restricted only by the local CFL condition. Thus each cell converges toward steady state at its own pace. In the converged steady-state solution, however, the numerical fluxes and sources exactly cancel, so the time step becomes irrelevant. The advantage of local time stepping is that it is very simple to implement, no extra calculations are needed, and the achieved acceleration can be similar or even better than with the artificial reduction of the speed of light. The disadvantage of local time stepping is that it cannot be applied to time-accurate runs at all, not even as a crude approximation.

Another way to accelerate the convergence to steady state is implicit time stepping. Implemention of a fully implicit MHD scheme is a nontrivial problem. The achievable acceleration strongly depends on the efficiency of the numerical schemes and the nonlinear instabilities of the simulated problem. The advantage of implicit time stepping is that it can be applied to time-accurate problems without changing the governing physical equations. The implementation of implicit time stepping into BATS-R-US is under development.

ACKNOWLEDGMENTS

This work was supported by the NSF KDI Grant NSF ATM-9980078, by NSF CISE Grant ACI-9876943 by DoD MURI Grant F49620-01-1-0359, and by NASA AISRP Grant NAG5-9406. GT has been partly supported by the Education Ministry of Hungary (Grant FKFP-0242-2000) and the Hungarian Science Foundation (OTKA, Grant D 25519).

REFERENCES

1. D. S. Balsara and D. S. Spicer, Maintaining pressure positivity in magnetohydrodynamic simulations, *J. Comput. Phys.* **148**, 133 (1999).
2. J. P. Boris, *A physically Motivated Solution of the Alfvén Problem*, Tech. Report NRL Memorandum Report 2167 (Naval Research Laboratory, Washington, DC, 1970).
3. P. J. Dellar, A note on magnetic monopoles, dimensional splitting, and the MHD Riemann problem, *J. Comput. Phys.* **172**, 392 (2001).
4. C. R. Evans and J. F. Hawley, Simulation of magnetohydrodynamic flows: A constrained transport method, *Astrophy. J.* **332**, 659 (1998).
5. S. K. Godunov, Symmetric form of the equations of magnetohydrodynamics, in *Numerical Methods for Mechanics of Continuum Medium* (Siberian Branch of USSR Acad. of Sci., 1972), Vol. 1, pp. 26-34 (in Russian).
6. C. Hirsch, *Numerical Computation of Internal and External Flows Volume 2, Computational Methods for Inviscid and Viscous Flows* (Wiley, Toronto, 1990).
7. P. Janhunen, A positive conservative method for magnetohydrodynamics based on HLL and Roe methods, *J. Comput. Phys.* **160**, 649 (2000).
8. F. Jüttner, Das Maxwellsche Gesetz der Geschwindigkeitsverteilung in der Relativtheorie, *Ann. Phys.* **34**, 856 (1911).
9. S. Koide, K. Nishikawa, and T. L. Mutel, A two-dimensional simulation of a relativistic magnetized jet, *Astrophys. J.* **463**, L71 (1996).
10. L. D. Landau and E. M. Lifshitz, The Classical Theory of Fields, 4th ed. (Pergamon Press, Oxford, England, 1975).
11. L. D. Landau and E. M. Lifshitz, Fluid Mechanics, 2nd ed. (Pergamon Press, Oxford, England, 1987).
12. T. J. Linde, *A Three-Dimensional Adaptive Multifluid MHD Model of the Heliosphere*, Ph.D. thesis (Univ. of Michigan, Ann Arbor, 1998).
13. J. G. Lyon, J. A. Fedder, and J. G. Huba, The effect of different resistivity models on magnetotail dynamics, *J. Geophys, Res.* **91**, 8057 (1988).

14. B. Marder, A method for incorporating Gauss' law into electromagnetic PIC codes, *J. Comput. Phys.* **68**, 48 (1987).
15. T. Ogino and R. J. Walker, A magnetohydrodynamic simulation of the bifurcation of tail lobes during intervals with a northward interplanetary magnetic field, *Geophys. Res. Lett.* **11**, 1018 (1984).
16. K. G. Powell, An Approximate Riemann Solver for Magnetohydrodynamics (*That Works in More Than One Dimension*), Tech. Report 94-24 (Inst. for Comput. Appl. in Sci. and Eng., NASA Langley Space Flight Center, Hampton, VA, 1994).
17. K. G. Powell, P. L. Roe, T. J. Linde, T. I. Gombosi, and D. L. De Zeeuw, A solution-adaptive upwind scheme for ideal magnetohydrodynamics, *J. Comput. Phys.* **154**, 284 (1999).
18. J. Raeder, R. J. Walker, and M. Ashour-Abdalla, The structure of the distant geomagnetic tail during long periods of northward IMF, *Geophys. Res. Lett.* **22**, 349 (1995).
19. P. L. Roe and D. S. Balsara, Notes on the eigensystem of magnetohydrodynamics, *SIAM J. Appl. Math.* **56**, 57 (1996).
20. T. Tanaka, Finite volume TVD scheme on an unstructured grid system for three-diemensional MHD simultions of inhomogeneous systems including strong background potential field, *J. Comput. Phys.* **111**, 381 (1994).
21. G. Tóth, The $\nabla \cdot \mathbf{B}$ constraint in shock capturing magnetohydrodynamic codes, *J. Comput. Phys.* **161**, 605 (2000).
22. G. Tóth and D. Odstrcil, Comparison of some flux corrected transport and total variation diminishing numerical schemes for hydrodynamic and magnetohydrodynamic problems, *J. Comput. Phys.* **128**, 82 (1996).
23. W. W. White, G. L. Siscoe, G. M. Erickson, Z. Kaymaz, N. C. Maynard, K. D. Siebert, B. U. Ö. Sonnerup, and D. R. Weimer, The magnetospheric sash and the cross-tail S, *Geophys. Res. Lett.* **25**, 1605 (1998).